European Journal of Medicinal Chemistry 224 (2021) 113671

Contents lists available at ScienceDirect

European Journal of Medicinal Chemistry

journal homepage: http://www.elsevier.com/locate/ejmech

Discovery of penipanoid C-inspired 2-(3,4,5-trimethoxybenzoyl) quinazolin-4(3*H*)-one derivatives as potential anticancer agents by inhibiting cell proliferation and inducing apoptosis in hepatocellular carcinoma cells

Chao-Jie Wang [a, b, 1], Xinxin Guo [a, b, 1], Rui-Qin Zhai [a, b], Changning Sun [a, b], Guokai Xiao [a, b], Jin Chen [a, b], Mei-Yan Wei [a, c], Chang-Lun Shao [a, b, *], Yuchao Gu [a, b, **]

[a] *Key Laboratory of Marine Drugs, The Ministry of Education of China, School of Medicine and Pharmacy, Ocean University of China, Qingdao, 266003, People's Republic of China*

[b] *Laboratory for Marine Drugs and Bioproducts of Pilot National Laboratory for Marine Science and Technology (Qingdao), Qingdao, 266237, People's Republic of China*

[c] *College of Food Science and Engineering, Ocean University of China, Qingdao, 266003, People's Republic of China*

ARTICLE INFO

Article history:
Received 1 April 2021
Received in revised form
22 June 2021
Accepted 24 June 2021
Available online 30 June 2021

Keywords:
Hepatocellular carcinoma
Penipanoid C
Quinazoline
Apoptosis
Cell cycle

ABSTRACT

Hepatocellular carcinoma (HCC) is the most common form of liver cancer and the fourth leading cause of cancer-related death worldwide. First-line drugs such as sorafenib provide only a modest benefit to HCC patients. In this study, the gram-scale synthesis of 2-benzoylquinazolin-4(3*H*)-one skeleton was achieved successfully via the I_2/DMSO catalytic system. A series of penipanoid C-inspired 2-(3,4,5-trimethoxybenzoyl)quinazolin-4(3*H*)-one derivatives was synthesized and evaluated for their cytotoxic activities against four cancer cell lines, HepG2, Bel-7402, A549, and U251. Among these compounds, **4a** was the most effective one with IC_{50} values of 1.22 μM and 1.71 μM against HepG2 and Bel-7402 cells, respectively. Mechanistic studies showed that **4a** inhibited hepatocellular carcinoma cell proliferation via arresting cell cycle. Additionally, **4a** induced HepG2 cells apoptosis by inducing reactive oxygen species production and elevating the expression of apoptosis-related proteins. More importantly, **4a** displayed significant *in vivo* anticancer effects in the HepG2 xenograft models. This suggests that **4a** is a promising lead compound with the potential to be developed as a chemotherapy agent for hepatocellular carcinoma.

1. Introduction

Liver cancer remains a global health challenge, with an estimated incidence of >1 million cases by 2025 [1]. Hepatocellular carcinoma (HCC) is the most common form of liver cancer and the fourth leading cause of cancer-related death worldwide [1]. First-line drugs such as sorafenib provide only a modest benefit to HCC patients [2]. Therefore, there is an urgent task for researchers to discover novel molecules for HCC patients. Marine natural products are an alternative resource for new drugs used to combat major diseases [3]. Several marine drugs have been successfully marketed, including the anticancer drug ET743 (Yondelis®) [3].

Quinazoline is a core structure in a large variety of compounds that exhibited a diverse biological activities, such as anticancer [4], anti-inflammatory [5], anti-tuberculosis [6], anti-pulmonary fibrosis [7], and anti-viral [8]. Especially, a large number of quinazoline derivatives have been studied for their anticancer activities over the years. In our previous research, a series of bioactive natural products were isolated from marine-derived fungi [9–12]. The quinazoline-containing natural alkaloid, penipanoid C (Fig. 1) was reported first from *Penicillium paneum* SD-44 [13], and re-isolated from the organic crude extraction of the marine-derived

* Corresponding author. Key Laboratory of Marine Drugs, The Ministry of Education of China, School of Medicine and Pharmacy, Ocean University of China, Qingdao, 266003, People's Republic of China.

** Corresponding author. Key Laboratory of Marine Drugs, The Ministry of Education of China, School of Medicine and Pharmacy, Ocean University of China, Qingdao, 266003, People's Republic of China.

E-mail addresses: shaochanglun@163.com (C.-L. Shao), guych@126.com (Y. Gu).

[1] These authors contributed equally to this work.

https://doi.org/10.1016/j.ejmech.2021.113671
0223-5234/

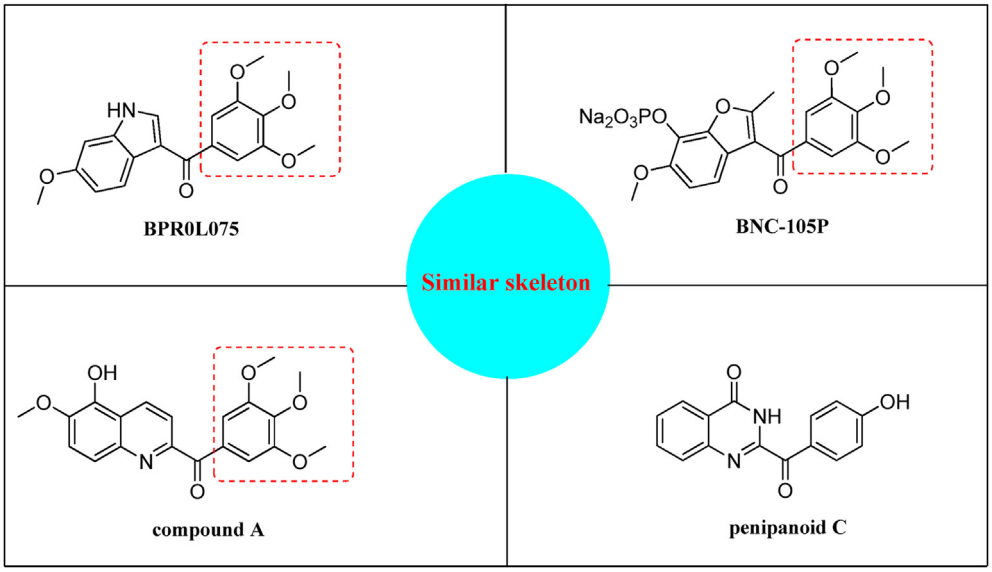

Fig. 1. Structures of compound A, BPR0L075, BNC-105P and penipanoid C.

Penicillum sp. CHNSCLM-0019 fungus in our laboratory.

The structural skeleton of penipanoid C is 2-benzoylquinazolin-4(3*H*)-one. The gram-scale synthesis of the skeleton of penipanoid C and the anticancer activity of its derivatives has not been reported before. Therefore, our research aims to synthesize and functionalize the 2-benzoylquinazolin-4(3*H*)-one skeleton at gram-scale followed by anticancer activity evaluation of the derivatives. How to perform the structural modification? It has to be noticed that the structural skeleton of penipanoid C is similar to some anticancer agents, such as compound A [14], BPR0L075 [15], and BNC-105P [16] (Fig. 1). Moreover, the 3,4,5-trimethoxyphenyl (TMP) moiety is an essential active group for these anticancer agents [14–16]. Inspired by this, the 4-hydroxyphenyl group in penipanoid C was replaced with a TMP group, followed by structural modifications at different sites to obtain a series of 2-(3,4,5-trimethoxybenzoyl)-quinazolin-4(3*H*)-one derivatives (Fig. 2).

The gram-scale synthesis of 2-benzoylquinazolin-4(3*H*)-one skeleton was successfully realized via the I_2/DMSO catalytic system, and then a series of penipanoid C-inspired 2-(3,4,5-trimethoxybenzoyl)-quinazolin-4(3*H*)-one derivatives were synthesized and evaluated for their cytotoxic activities against four cancer cell lines, including hepatocellular carcinoma HepG2/Bel-7402 cells, human lung cancer cells A549, and human glioma cells U251. The most effective compound, **4a**, notably inhibited the proliferation of hepatocellular carcinoma cells. Additionally, the roles and mechanisms of **4a** in anticancer activity were investigated in both hepatocellular carcinoma cellular and mouse xenograft models. The results indicated that **4a** is a potentially promising lead compound for hepatocellular carcinoma therapy.

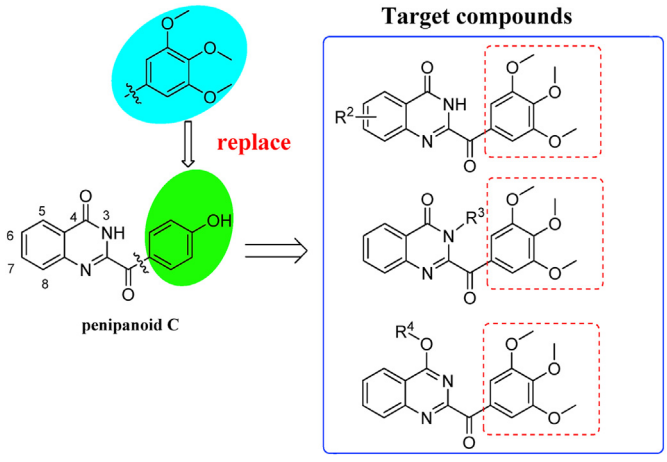

Fig. 2. Design strategy for novel 2-(3,4,5-trimethoxybenzoyl)quinazolin-4(3*H*)-one derivatives as anticancer agents.

2. Results and discussion

2.1. Chemistry

Two classic methods based on oxidative coupling reaction were reported to synthesize 2-benzoylquinazolin-4(3*H*)-one derivatives. Firstly, the Wu group reported an I_2/DMSO promoted oxidative coupling reaction between 2-aminobenzamides with acetophenones to provide various 2-benzoylquinazolin-4(3*H*)-ones [17]. Secondly, the Nguyen group demonstrated recently a new method to access 2-benzoylquinazolin-4(3*H*)-ones utilizing sulfur [18]. The advantage of Wu's reaction strategy is the rapid synthesis of the target product in an atom- and step-economic fashion. However, when there is no substituent on the benzene ring of 2-aminobenzamide, the by-product 2-benzoyl-6-iodoquinazolin-4(3*H*)-one analogue is easily produced and difficult to remove. The advantage of Nguyen's reaction strategy is the wide range of substrate applicability, while the disadvantage is the long reaction time. Neither reaction strategy has studied the gram-scale synthesis of the 2-benzoylquinazolin-4(3*H*)-one skeleton.

The optimization studies of the synthesis of penipanoid C at 100 mg level based on oxidative coupling reaction were executed (Table 1). Initially, we tried the reaction of 2-aminobenzamide **1a** with 4′-hydroxyacetophenone **2a** in the presence of 300 mol % SeO_2, 400 mol % H_2SO_4, in 4 mL of DMSO, at 100 °C. To our disappointment, the reaction was significantly less effective (Table 1, entry 1). In the absence of the H_2SO_4, no desired product was detected (Table 1, entry 2). The catalyst Se, was also studied and unfortunately, no good yields of penipanoid C were obtained (Table 1, entries 3–5). The formation of penipanoid C was observed when Nguyen's reaction method was used (23–26%, Table 1, entries

Table 1
Optimization of reaction for the synthesis of penipanoid C.

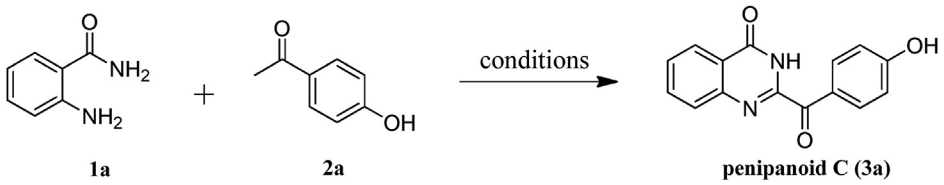

entry	cat.(mol %)	additive (mol %)	solvent	Temp (°C)	Time (h)	Yield (%)[c]
1[a]	SeO_2 (300)	H_2SO_4 (400)	DMSO	100	24	<5
2[a]	SeO_2 (300)	–	DMSO	100	24	0
3[a]	Se (400)	*N*-methylpiperidine (100)	DMSO	110	48	0
4[a]	Se (400)	H_2SO_4 (400)	DMSO	130	48	0
5[a]	Se (400)	CH_3COOH (400)	DMSO	160	48	0
6[a]	S_8 (400)	*N*-methylpiperidine (100)	DMSO	100	24	23
7[a]	S_8 (400)	*N*-methylpiperidine (100)	DMSO	110	24	26
8[b]	I_2 (110)	–	DMSO	110	2	48

[a] A mixture of 2-aminobenzamide **1a** (1 mmol), 4′-hydroxyacetophenone **2a** (1 mmol), catalyst, additive, were heated in DMSO (4 mL).
[b] A mixture of 4′-hydroxyacetophenone **2a** (1 mmol) and I_2 (1.1 mmol) in DMSO (2 mL) was stirred at 110 °C, and then 2-aminobenzamide **1a** (1 mmol in 2 mL DMSO) was added slowly dropwise to the mixture during 0.5 h.
[c] Isolated yield.

Table 2
Gram-scale synthesis of penipanoid C derivatives (**3a**–**3i**)[a] and their cytotoxic activities *in vitro*[b].

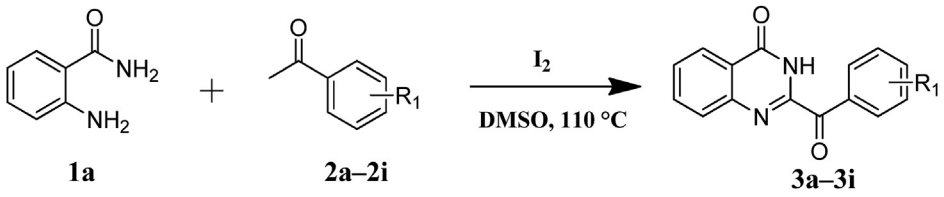

entry	Product	R_1	Mass (g)	Yield (%)[c]	IC_{50} (μM)
1	**3a**	4-OH	1.22	31	>50
2	**3b**	4-OCH_3	2.47	60	>50
3	**3c**	2-OCH_3	2.62	64	>50
4	**3d**	4-F	2.78	71	>50
5	**3e**	4-Cl	3.21	77	>50
6	**3f**	4-OCF_3	1.83	37	>50
7	**3g**	2-OCF_3	1.92	39	>50
8	**3h**	4-CF_3	1.94	42	>50
9	**3i**	2-CF_3	1.86	40	>50

[a] Reaction condition: A mixture of **2a**–**2i** (14.69 mmol) and I_2 (16.16 mmol) in DMSO (10 mL) was stirred at 110 °C, and then 2-aminobenzamide **1a** (14.69 mmol in 15 mL DMSO) was added slowly dropwise to the mixture during 7.5 h.
[b] HepG2 cell line.
[c] Isolated yield.

6–7). Finally, the reaction worked even better with Wu's reaction conditions (48%, Table 1, entry 8).

With the optimized conditions (Table 1, entry 8) in hand, the gram-scale synthesis of penipanoid C was carried out. Preliminary experiments showed that the addition rate of compound **1a** was critical for the gram-scale reaction and affected the production of by-product 2-(4-hydroxybenzoyl)-6-iodoquinazolin-4(3*H*)-one (data not shown); the gram-scale synthesis of penipanoid C gave a yield of 31% at an optimal addition rate of 4.44 mg/min (Table 2, entry 1). Therefore, the applicability of the scope of diversely acetophenone analogues **2b**–**2i** was explored. The reactions proceeded smoothly for the corresponding penipanoid C derivatives (**3b**–**3i**) in acceptable to moderate isolated yields (Table 2, 37–77%). Generally, acetophenone analogues *p*-substituted by an electron-donating or halogen group gave better yields (Table 2, entries 2–5). On the other side, acetophenone analogues *o*- or *p*-substituted by an electron-withdrawing group lowered the yields (Table 2, entries 1 and 6–9).

After completing the gram-level synthesis of 2-benzoylquinazolin-4(3*H*)-one skeleton, a series of 2-(3,4,5-trimethoxybenzoyl)quinazolin-4(3*H*)-one derivatives were synthesized (Scheme 1). The synthesis of **4a**–**4u** is similar to that of penipanoid C. Compound **4a** was reacted with the appropriate halogenated compounds in the presence of K_2CO_3 to give the target products **5a**–**5c** and **8a**–**8d**. Treatment of **4a** with BOP, DBU, and suitable alcohols in refluxing acetonitrile produced **6a**–**6b**. Compound **4a** was chlorinated by phosphorus oxychloride to afford **9** in 85% yield.

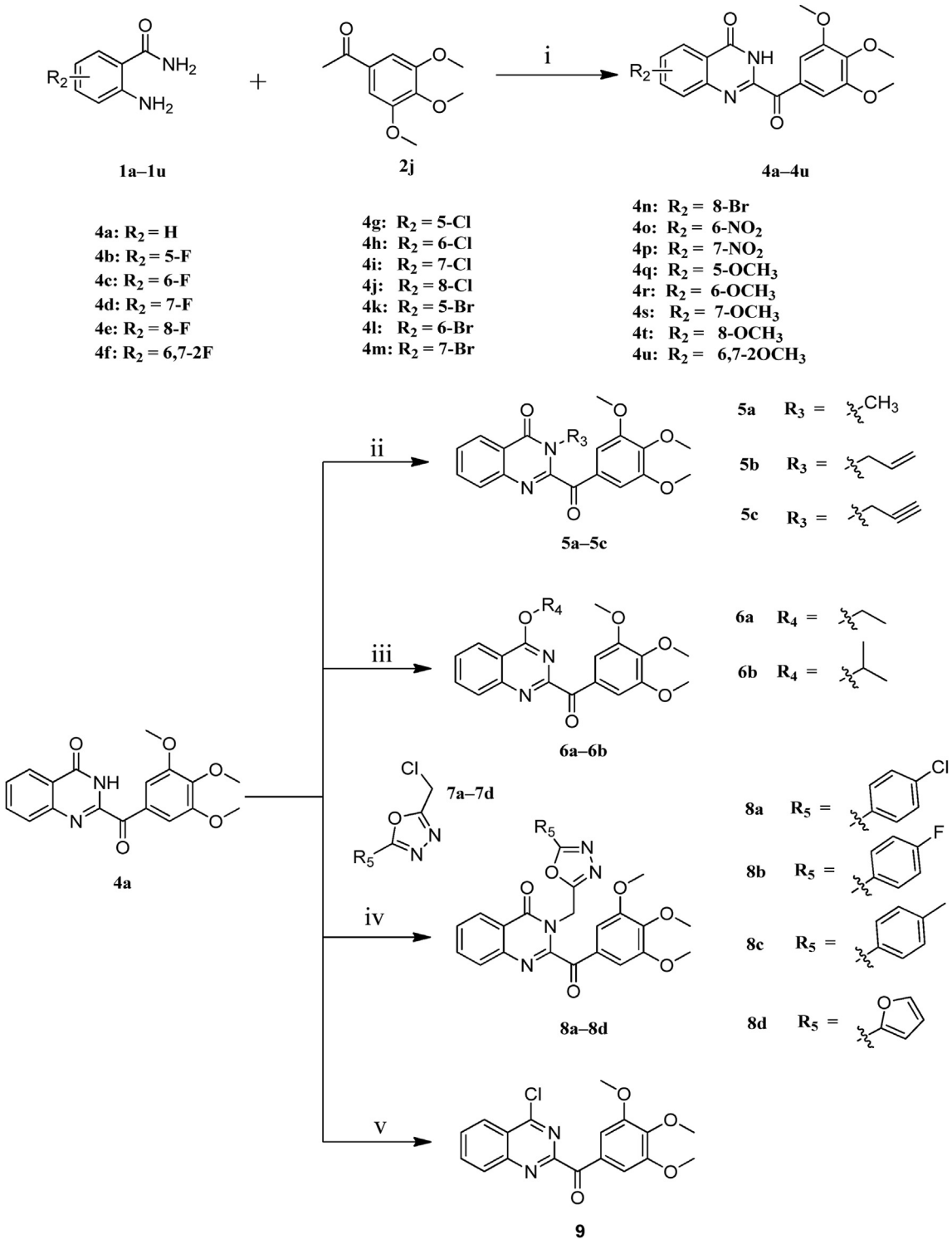

Scheme 1. Synthesis of 2-(3,4,5-trimethoxybenzoyl)quinazolin-4(3*H*)-one derivatives. Reagents and conditions: (i) I_2, DMSO, 110 °C, 1.5 h; (ii) R_3X (X = I or Br), K_2CO_3, DMF, 80 °C, 12 h; (iii) R_4OH, BOP, DBU, CH_3CN, 85 °C, 48 h; (iv) **7a**–**7d**, K_2CO_3, DMF, 80 °C, 12 h; (v) $POCl_3$, 100 °C, 1 h.

2.2. Biological assays

2.2.1. Cytotoxic activity of 2-(3,4,5-trimethoxybenzoyl)quinazolin-4(3H)-one derivatives and structure-activity relationships analysis

The results of the titled compounds (**4a**–**4u**, **5a**–**5c**, **6a**–**6b**, **8a**–**8d**, **9**) against HepG2 cancer cells at 2.5 μM are present in Fig. 3. The compounds with the inhibition rate of more than 10% were considered acceptable. Therefore, **4a**, **4m**, **4q**, **4s**, **5a**–**5c**, **6a**–**6b**, **8b**–**8d**, and **9** were evaluated for their cytotoxic activity against another three cancer cell lines (Bel-7402, A549, and U251) with Adriamycin as positive control (Table 3). The results showed that **4a** was the most effective compound against all four cancer cell lines with the IC_{50} values ranging from 1.22 to 5.48 μM.

Compounds **3a**–**3i** showed no apparent inhibitory effects against HepG2 cells (IC_{50} > 50 μM, Table 2). However, **4a** exhibited good inhibitory activity against HepG2 with the IC_{50} value of

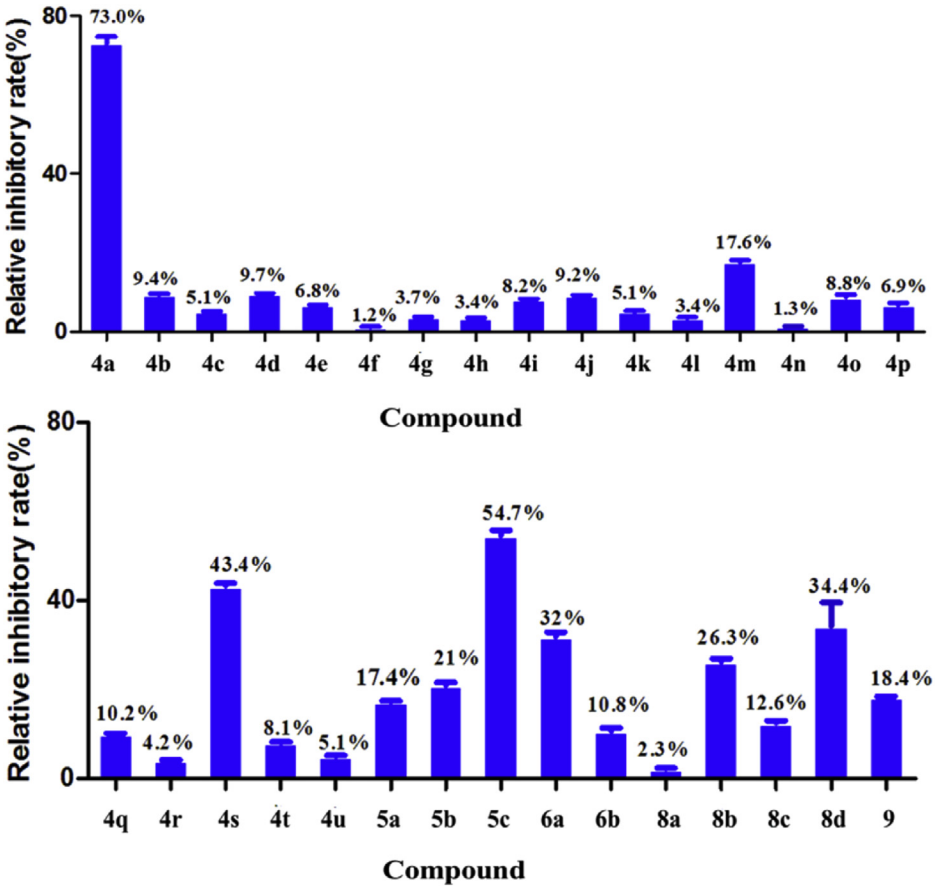

Fig. 3. *In vitro* cytotoxic activity of 2-(3,4,5-trimethoxybenzoyl)quinazolin-4(3*H*)-one derivatives against HepG2 cells. HepG2 cells were treated with the compounds at 2.5 μM, and then inhibition rates were determined by the MTT assay at 72 h. Inhibition rates are presented as mean ± standard error of mean, n = 5.

Table 3
The cytotoxicity data of 2-(3,4,5-trimethoxybenzoyl)quinazolin-4(3*H*)-one derivatives in cancer cell lines[a].

Compounds	IC_{50} (μmol/L)					
	HepG2	Bel-7402	A549	U251	NCI−H1299	HCT116
4a	**1.22 ± 0.12**	**1.71 ± 0.18**	**3.88 ± 0.22**	**5.48 ± 0.29**	**13.94 ± 2.26**	**5.47 ± 0.11**
4m	7.45 ± 0.41	4.91 ± 0.19	7.27 ± 0.19	>100	NT[b]	NT[b]
4q	9.15 ± 0.21	7.1 ± 0.31	15.42 ± 0.87	19.16 ± 0.85	NT[b]	NT[b]
4s	10.62 ± 0.38	4.13 ± 0.16	12.73 ± 0.68	13.69 ± 0.79	NT[b]	NT[b]
5a	8.19 ± 0.19	6.34 ± 0.12	20.26 ± 1.08	>100	NT[b]	NT[b]
5b	14.10 ± 0.35	10.70 ± 0.56	10.52 ± 0.63	12.99 ± 0.91	NT[b]	NT[b]
5c	4.97 ± 0.17	5.40 ± 0.24	7.66 ± 0.28	12.82 ± 1.07	NT[b]	NT[b]
6a	15.55 ± 1.03	8.29 ± 0.24	>100	10.57 ± 0.63	NT[b]	NT[b]
6b	7.45 ± 0.41	4.91 ± 0.19	7.27 ± 0.19	>100	NT[b]	NT[b]
8b	7.07 ± 0.16	4.86 ± 0.15	7.66 ± 0.31	27.46 ± 1.45	NT[b]	NT[b]
8c	10.47 ± 0.32	8.88 ± 0.32	47.13 ± 2.21	26.96 ± 1.72	NT[b]	NT[b]
8d	7.51 ± 0.16	8.15 ± 0.33	4.62 ± 0.21	15.93 ± 0.89	NT[b]	NT[b]
9	10.92 ± 0.25	6.88 ± 0.32	7.09 ± 0.34	>100	NT[b]	NT[b]
Adriamycin	2.21 ± 0.16	1.28 ± 0.12	2.19 ± 0.28	0.157 ± 0.07	NT[b]	NT[b]

[a] Each experiment was repeated at least three times independently.
[b] NT means not tested.

1.22 μM (Table 3), which suggested that the TMP moiety in **4a** is necessary for the cytotoxic activity. The activity decreased obviously when the halogen/electron-donating groups were substituted at the 6-position (Fig. 3, **4c/4h/4l/4r** vs **4a**). Compound **4a** exhibited better inhibitory activity than 3-substituted compounds **5a**−**5c** and **8a**−**8d** against four cancer cell lines (Table 3), this indicated that the substitute at 3-position (the NH group) of **4a** may play a critical role in the cytotoxic activity. A summary of the structure−activity relationships was shown in Fig. 4.

It had to be noticed that **4a**, **4q**, **4s**, **5a**, **5c**, **8b**, and **8c** exhibited stronger proliferation inhibition effects on hepatocellular carcinoma HepG2 and Bel-7402 cell lines than non-hepatocellular carcinoma cell lines of A549 and U251. Therefore, the cytotoxic activity of **4a** was further evaluated against two other non-hepatocellular carcinoma cell lines, including human lung cancer cell NCI−H1299 (IC_{50} 13.94 μM) and human colon cancer cell HCT116 (IC_{50} 5.47 μM). Compound **4a** showed strong cytotoxic activity against HepG2 and Bel-7402 cells with IC_{50} values lower than 2 μM.

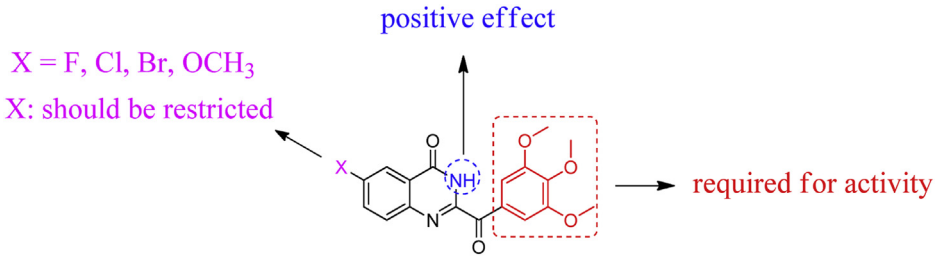

Fig. 4. Structure–activity relationships of 2-(3,4,5-trimethoxybenzoyl)quinazolin-4(3*H*)-one derivatives as anticancer agents.

Table 4
The cytotoxicity data of compound **4a** in cancer cell lines and normal cell lines.

Compound	IC_{50} (μmol/L)		SI
	HepG2	L-O2	
4a	**1.22 ± 0.12**	**6.01 ± 0.31**	**4.9**

SI: selectivity index (IC_{50} on L-O2 cells/IC_{50} on HepG2 cells).

But, **4a** displayed at least two times decreased potency against four non-hepatocellular carcinoma cell lines (IC_{50} 3.88–13.94 μM). These results suggested that **4a** exhibited stronger inhibition of the proliferation of hepatocellular carcinoma cell lines than non-hepatocellular carcinoma cell lines. Compound **4a** was further tested against normal L-O2 cells (Table 4).

2.2.2. Compound *4a* inhibits colony formation of hepatocellular carcinoma cells

Colony formation assay was used to evaluate the proliferation and survival abilities of a single adherent cell [19,20]. Compound **4a** was chosen to test its inhibitory effects on colony formation assay. HepG2 and Bel-7402 cells were treated with **4a** at concentrations of 0.2, 0.4, 0.8, 1.6, and 3.2 μM for 10 days, respectively. As shown in Fig. 5, 1.6 μM of **4a** suppressed the colony formation of HepG2 and Bel-7402 cells effectively. Moreover, 3.2 μM of **4a** almost eliminated the colony formation. Compound **4a** displayed strong anti-proliferation effects on hepatocellular carcinoma cells. Therefore, the mechanisms of anticancer activity of **4a** in hepatocellular carcinoma cells were further investigated.

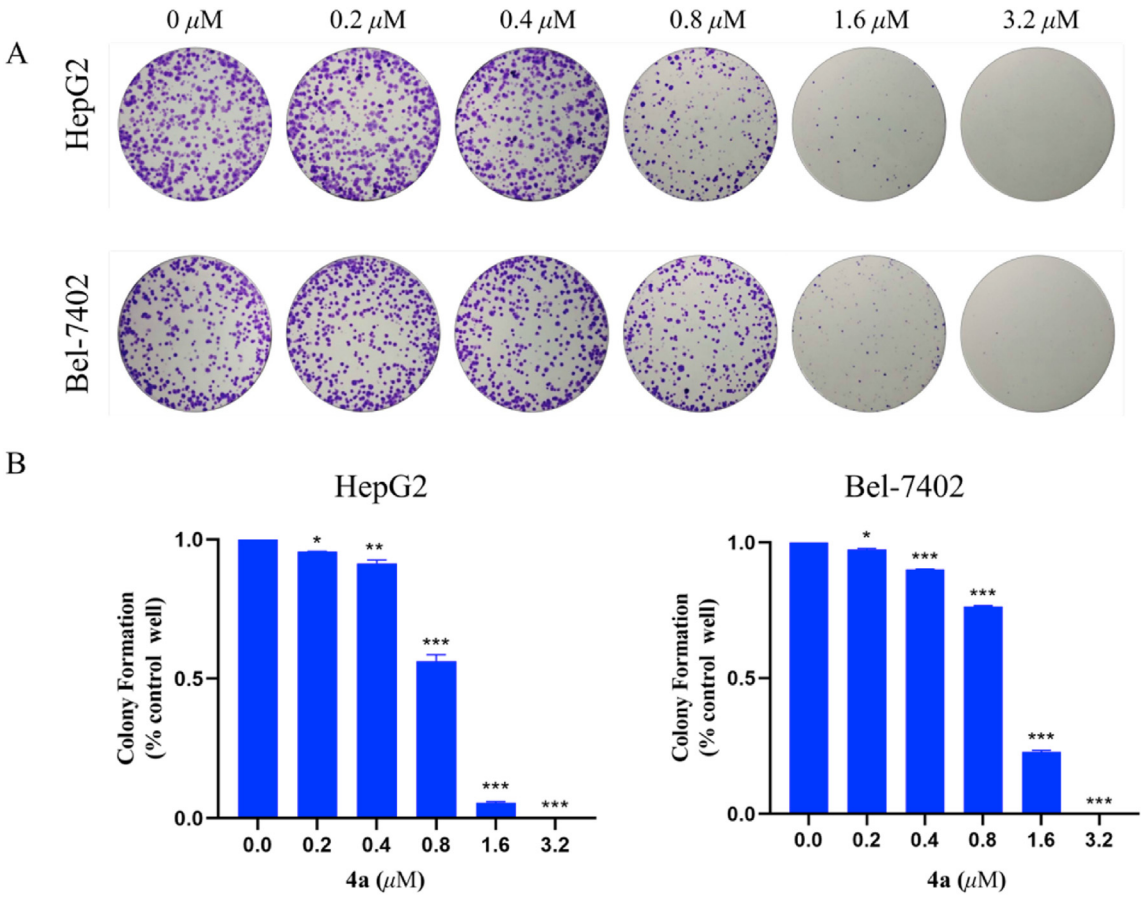

Fig. 5. Colony formations of HepG2 and Bel-7402 cells were inhibited by compound **4a**. (A) HepG2 and Bel-7402 cells were cultured for 10 days with varying concentrations of compound **4a** (0, 0.2, 0.4, 0.8, 1.6, 3.2 μM) and the colonies were fixed and dyed with 0.1% crystal violet. (B) The relative colony numbers were shown in histograms. Error bars are the SD, n = 3. Statistical significance of differences in mean values are $^{*}p < 0.05$ and $^{***}p < 0.001$.

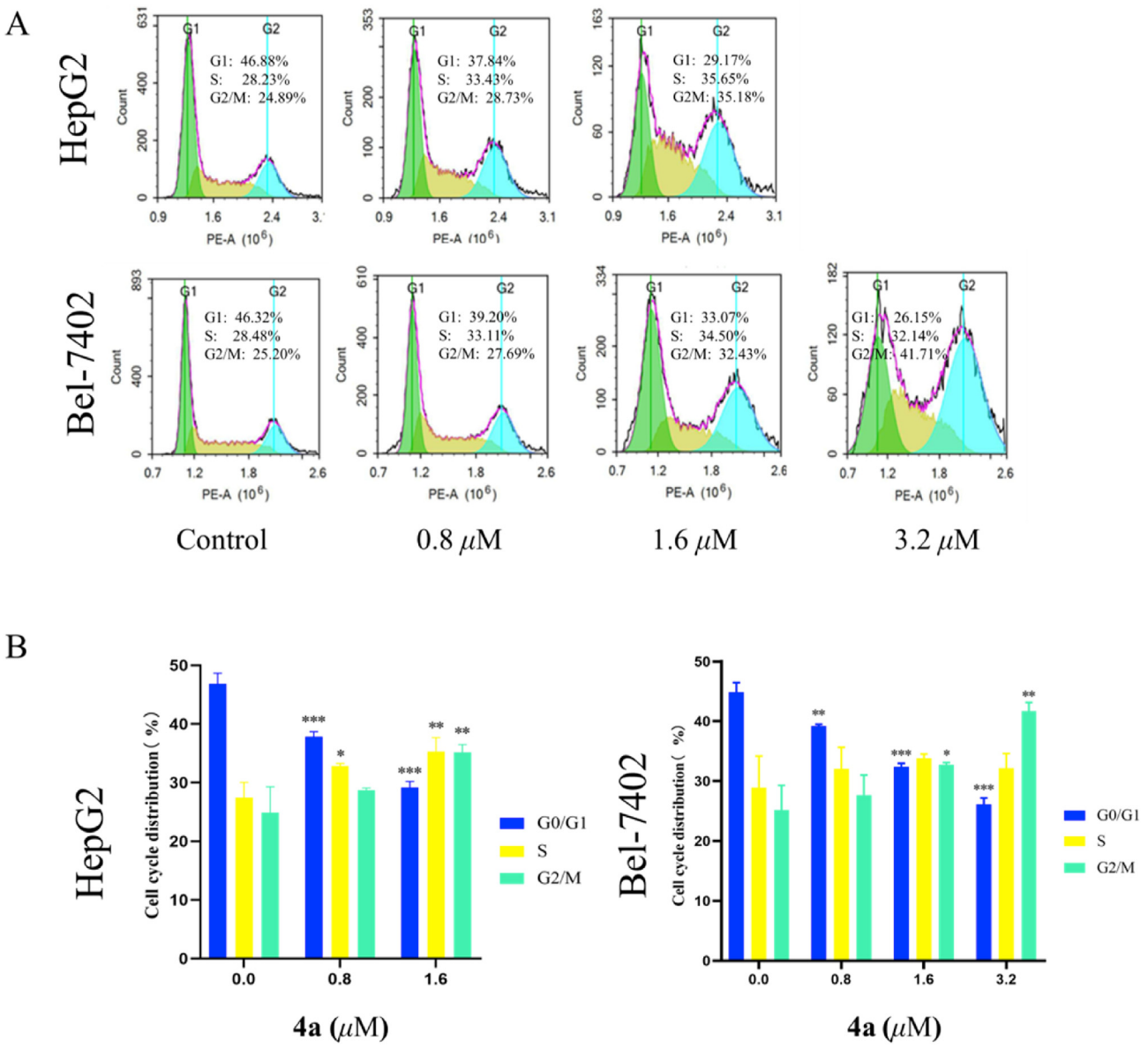

Fig. 6. Compound **4a** induced cell cycle arrest in HepG2 and Bel-7402 cells. (A) HepG2 and Bel-7402 cells were incubated respectively with varying concentrations of compound **4a** (0, 0.8, 1.6, 3.2 μM) and analyzed by flow cytometry. (B) Histograms displaying the percentage of cell cycle distribution. Error bars are the SD, n = 3. Statistical significance of differences in mean values are $^{*}p < 0.05$, $^{**}p < 0.01$ and $^{***}p < 0.001$.

2.2.3. Compound ***4a*** blocks the cell cycle and regulates the expression of proliferation-related proteins

Cell cycle is the basis of cell life activity and controls the entry of stationary phase cells into the proliferative phase [21,22]. A cell-cycle cytotoxicity assay was performed by treating HepG2 and Bel-7402 cells at various concentrations of **4a** (0, 0.8, 1.6, and 3.2 μM) for 48 h, respectively. However, after incubating with compound **4a** at 3.2 μM for 48 h, most of the HepG2 cells died, making the result unavailable. The cell cycle of HepG2 cells was significantly arrested at the S and G2/M phase. The percentage of cells in the S stage increased from 28.23% to 35.65% (Fig. 6). The percentage of cells in the G2/M stage increased from 24.89% to 35.18% (Fig. 6). The cell cycle of Bel-7402 cells was arrested at the G2/M phase, the percentage of cells in the G2/M stage increased from 25.20% to 41.71% (Fig. 6). These results indicated that **4a** induced cell cycle arrest in both HepG2 and Bel-7402 cells.

Since PI3K/AKT and MAPK/ERK1/2 are important signaling pathways mediating the cell proliferation response [23,24], the effects of **4a** on AKT and ERK1/2 phosphorylation were examined by Western blot. Treatment of HepG2 cells with **4a** resulted in the down-regulation of phosphorylation levels of AKT and ERK1/2 in a dose-dependent manner (Fig. 7). Treatment of Bel-7402 cells with **4a** resulted in the down-regulation of phosphorylation levels of AKT and the up-regulation of phosphorylation levels of ERK1/2 in a dose-dependent manner (Fig. 7). These results suggested that the inhibition of the AKT signaling pathway might be the reason for cell cycle arresting of hepatocellular carcinoma cells by **4a**.

2.2.4. Compound ***4a*** induces apoptosis of HepG2 cells

HepG2 cells were cultured in a DMEM medium containing different concentrations of **4a** (0, 0.8, 1.6, 3.2 μM) for 48 h. Hoechst 33342 staining was used to assess nuclear changes in HepG2 cells. The chromatin was markedly shrunk after incubating with **4a** (Fig. 8A), indicating that the cells were undergoing apoptosis. The

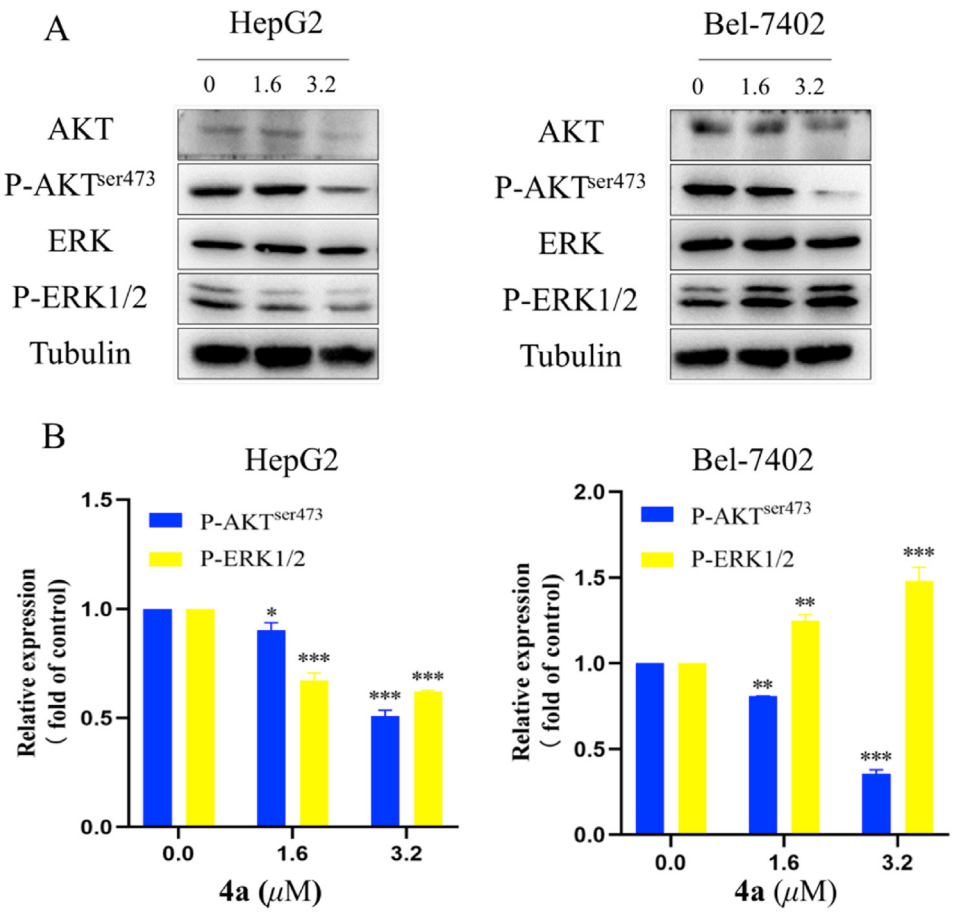

Fig. 7. Compound **4a** regulates the expression and activity of AKT and ERK1/2. (A) Western blot for AKT, *p*-AKT, ERK and *p*-ERK1/2 in HepG2 and Bel-7402 cells after incubated with the indicated concentrations of compound **4a** (0, 1.6, 3.2 μM) for 48 h. (B) The histograms are the quantification of AKT and ERK phosphorylation levels detected by Western blot in (A) (Control group set to 1). Error bars are the SD, n = 3. Statistical significance of differences in mean values are $^{*}p < 0.05$, $^{**}p < 0.01$ and $^{***}p < 0.001$.

apoptotic induction effects of **4a** were monitored by the Muse cell analyzer. The results showed that **4a** induced a dose-dependent increase (7.80−46.25%) of apoptosis of both early and late stages in HepG2 cells (Fig. 8B&C). Subsequently, Western blot analysis was carried out to examine the expression of apoptosis-related proteins (Fig. 8D&E). The expression of Cleaved-PARP and Cleaved-Caspase3 was significantly increased in HepG2 cells treated by **4a**. These data strongly demonstrated that **4a** could play anticancer roles by inducing cell apoptosis.

*2.2.5. Compound **4a** induced reactive oxygen species generation*

Reactive oxygen species (ROS) are chemically reactive molecules with essential functions in living organisms [25]. Excessive amounts of ROS cause oxidative damage to cells, and many chemotherapeutic drugs induce cancer cell apoptosis by generating ROS [26]. Therefore, the intracellular ROS production using fluorescence probe DCFH-DA was detected after treatment with different concentrations of **4a,** and then the accumulation of ROS was observed in a dose-dependent (Fig. 9). These data suggested that **4a** induced HepG2 cells apoptosis through the elevation of ROS levels.

*2.2.6. Compound **4a** suppresses the growth of xenograft tumors in nude mice*

Due to the remarkable antiproliferative and apoptosis induction activities of **4a** *in vitro*, its anticancer activity *in vivo* was assessed utilizing a mouse hepatic carcinoma cancer xenograft model established by the subcutaneous inoculation of HepG2 cells. Preliminary experiments showed that **4a** (5 mg/kg/d) could slightly but significantly inhibit tumor growth (data not shown). Therefore, 4 and 8 mg/kg of **4a** per day were used to assess its anticancer activity *in vivo*. The tumor volume (Fig. 10A) and body weight of nude mice (Fig. 10B) were monitored for 20 days. The low dose of **4a** (4 mg/kg) only slightly inhibited tumor growth inhibition (TGI = 19.11%) compared with the vehicle group (Fig. 10A). But, the high dose of compound **4a** (8 mg/kg) achieved significant tumor growth inhibition with a tumor growth inhibition (TGI) value of 67.57% (Fig. 10A). During the 20 days of treatment, all the animals in different treatment groups were kept at relatively stable body weight (Fig. 10B), suggesting the low toxicity of **4a**. After 20 days of drug treatment, the tumors were dissected and weighed (Fig. 10C&D), and the results were consistent with the tumor growth curves. Overall, these findings indicated that **4a** effectively inhibited cancer growth *in vivo* and represented a promising drug candidate for hepatocellular carcinoma.

3. Conclusion

In summary, this study has reported the gram-scale synthesis of 2-benzoylquinazolin-4(3*H*)-one skeleton utilizing the I_2/DMSO catalytic system and then identified penipanoid C-inspired anticancer agents that inhibit cell proliferation and induce apoptosis in hepatocellular carcinoma cells. Compound **4a**, notably inhibited the proliferation of hepatocellular carcinoma HepG2/Bel-7402 cells.

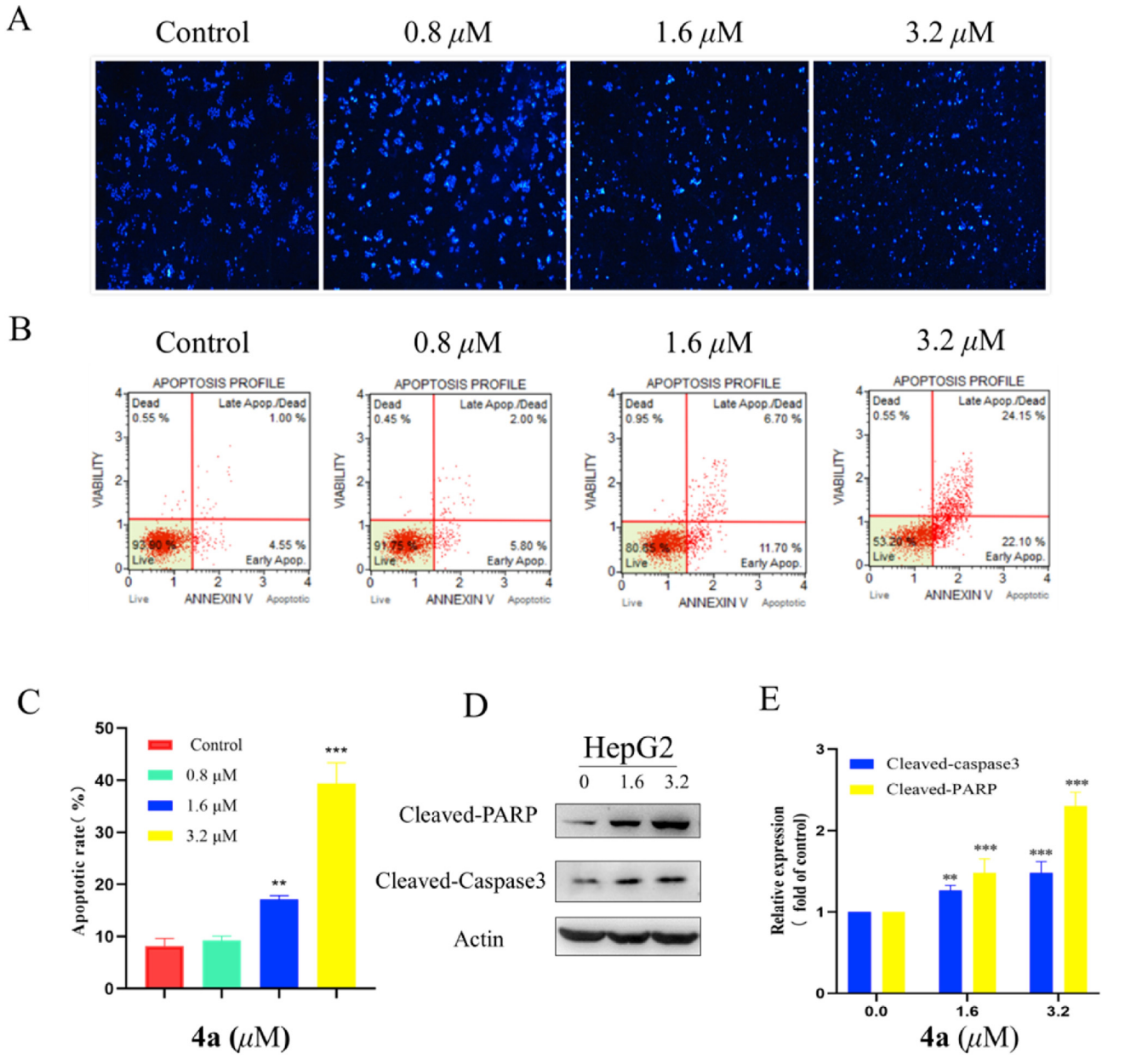

Fig. 8. Compound **4a** induced apoptosis of HepG2 cells. (A) HepG2 cell morphological changes after incubation with compound **4a**. (B) Different concentrations of compound **4a** (0.8, 1.6 and 3.2 μM) induced apoptosis in HepG2 cells. (C) Histograms display the percentage of cell distribution. Error bars are the SEM, n = 3. Statistical significance of differences in mean values are $*p < 0.05$, $**p < 0.01$ and $***p < 0.001$. (D) Western blot of apoptosis-related proteins in HepG2 cells after incubated with the indicated concentrations of compound **4a** (0, 1.6, 3.2 μM) for 48 h. (E) Quantification of Cleaved-PARP, Cleaved-Caspase3 is shown (Control group set to 1). Error bars are the SD, n = 3. Statistical significance of differences in mean values are $*p < 0.05$, $**p < 0.01$ and $***p < 0.001$.

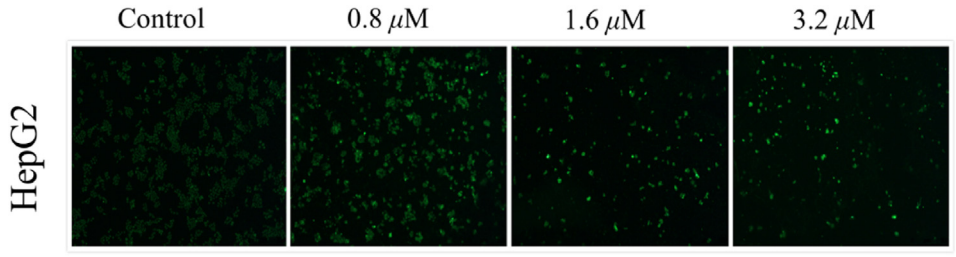

Fig. 9. Compound **4a** increased levels of ROS in HepG2 cells. The ROS levels of HepG2 cells were detected after incubated with different concentrations of compound **4a** (0, 0.8, 1.6, 3.2 μM).

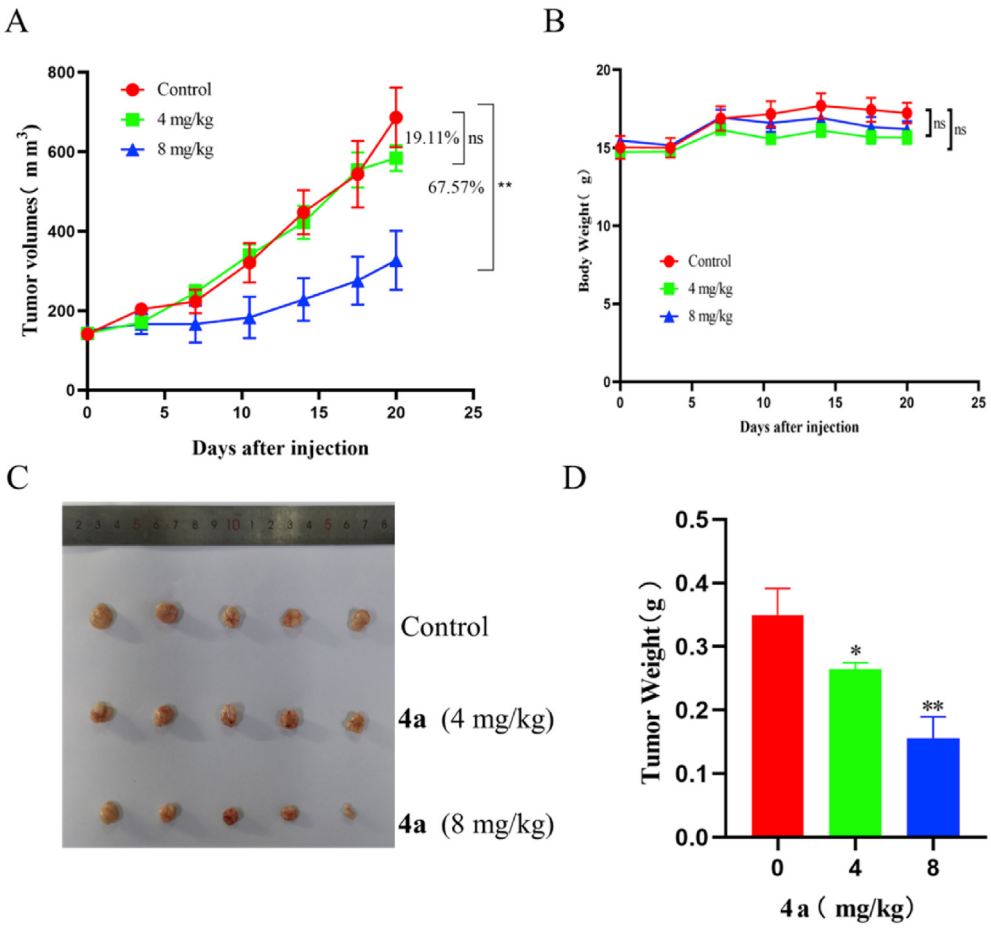

Fig. 10. Compound **4a** inhibits HepG2 xenograft growth *in vivo*. The mice bearing HepG2 xenograft tumors with the volumes of 100–200 mm^3 were randomly divided into 3 groups with 5 mice in each group. Mice were treated intraperitoneally with **4a** (4 mg/kg and 8 mg/kg) and control (15% *N*-Methyl pyrrolidone, 25% Solutol HS-15, 60% saline) once every days for 20 days. (A) The tumor volumes were examined twice a week. (B) Body weight changes of mice during treatment. (C) Visible tumor formation and photographs of representative tumors removed from mice at 20 days after initiation of treatment. (D) Compound **4a** treatment resulted in significantly lower tumor weight compared control. Error bars are the SEM, n = 3. Statistical significance of differences in mean values are $*p < 0.05$, $**p < 0.01$ and $***p < 0.001$.

The SAR results indicated that (1) the TMP moiety is necessary for the anticancer activity, (2) the halogen/electron-donating group substituted at the 6-position should be restricted, (3) the NH group at the 3-position is beneficial to anticancer activity. Mechanistic studies showed that **4a** inhibited hepatocellular carcinoma cell proliferation via arresting cell cycle. Additionally, compound **4a** induced HepG2 cancer cells apoptosis by inducing reactive oxygen species production and the expression of apoptosis-related proteins. Compound **4a** displayed significant *in vivo* anticancer effects in the HepG2 xenograft models, suppressing tumor growth by 67.57% at a dose of 8 mg/kg by ip injection every day for 20 days. Overall, these results demonstrated that **4a** is a potentially promising lead for hepatocellular carcinoma therapeutics.

4. Experimental section

4.1. Chemistry

Chemicals and solvents were purchased from commercial suppliers and were used without further purification. Thin-layer chromatography (TLC) was performed on silica gel 60 F254 (Qingdao Marine Chemical Ltd.). Column chromatography was performed over silica gel (200–300 mesh, Qingdao Marine Chemical Ltd.). ^{1}H NMR spectra were recorded on a Bruker 600 MHz and 400 MHz spectrometer, respectively (Bruker Company). ^{13}C NMR spectra were recorded on a Bruker 150 MHz, 125 MHz and 100 MHz spectrometer, respectively (Bruker Company). HRMS data were obtained using an APEX IV Fourier-Transform Mass Spectrometry (Bruker Company).

4.1.1. General procedures to synthesize ***3a*–*3i***

I_2 (1.1 eq) was added to a mixture of **2a**–**2i** (1 eq) and DMSO (10 mL). The solution was stirred at 110 °C, then 2-aminobenzamide (2.00 g, 14.69 mmol, 1 eq) in 15 mL DMSO was added dropwise to the mixture during 7.5 h. After the complete disappearance of the starting material, a sodium thiosulfate solution (1 g $Na_2S_2O_3$ in 60 mL water) was added dropwise to the reaction system. Filtrating and drying, the residue was purified by silica gel chromatography (petroleum ether/EtOAc 4:1) to yield the desired compounds.

*4.1.1.1. 2-(4-hydroxybenzoyl)quinazolin-4(3H)-one (**3a**).* Yellow solid, 1.22 g, yield 31%; ^{1}H NMR (400 MHz, DMSO-d_6, *J* in Hz) δ_H 12.59 (s, 1H), 10.77 (s, 1H), 8.20 (dd, $J = 8.0, 1.5$ Hz, 1H), 8.14–8.03 (m, 2H), 7.89 (ddd, $J = 8.5, 7.1, 1.6$ Hz, 1H), 7.78 (dd, $J = 8.3, 1.2$ Hz, 1H), 7.63 (ddd, $J = 8.0, 7.2, 1.2$ Hz, 1H), 7.12–6.62 (m, 2H). ^{13}C NMR (100 MHz, DMSO-d_6) δ_C 185.1, 163.6, 161.1, 149.9, 147.3, 134.8, 133.8, 128.2, 126.0, 125.2, 122.7, 115.5. HRESIMS *m/z* calcd for $C_{15}H_{11}N_2O_3^+$ 267.0764 $[M+H]^+$, found 267.0768.

*4.1.1.2. 2-(4-(methoxy)benzoyl)quinazolin-4(3H)-one (**3b**).* White solid, 2.47 g, yield 60%; ^{1}H NMR (400 MHz, DMSO-d_6, *J* in Hz) δ_H 12.61 (s, 1H), 8.30–8.11 (m, 3H), 7.89 (ddd, *J* = 8.5, 7.2, 1.6 Hz, 1H), 7.78 (dd, *J* = 8.2, 1.2 Hz, 1H), 7.65 (ddd, *J* = 8.1, 7.2, 1.2 Hz, 1H), 7.17–7.07 (m, 2H), 3.89 (s, 3H). ^{13}C NMR (100 MHz, DMSO-d_6) δ_C 185.8, 164.8, 161.5, 150.0, 147.7, 135.2, 133.9, 128.8, 128.7, 127.1, 126.5, 123.2, 114.6, 56.2. HRESIMS *m/z* calcd for $C_{16}H_{13}N_2O_3^+$ 281.0921 $[M+H]^+$, found 281.0925.

*4.1.1.3. 2-(2-(methoxy)benzoyl)quinazolin-4(3H)-one (**3c**).* White solid, 2.62 g, yield 64%; ^{1}H NMR (600 MHz, DMSO-d_6, *J* in Hz) δ_H 12.69 (s, 1H), 8.16 (dd, *J* = 7.9, 1.6 Hz, 1H), 7.83 (ddd, *J* = 8.4, 7.1, 1.6 Hz, 1H), 7.66–7.60 (m, 3H), 7.61 (ddd, *J* = 8.2, 7.1, 1.2 Hz, 1H), 7.19–7.16 (m, 1H), 7.14 (td, *J* = 7.5, 1.0 Hz, 1H), 3.63 (s, 3H). ^{13}C NMR (150 MHz, DMSO-d_6) δ_C 189.5, 161.6, 159.7, 151.3, 148.1, 135.4, 135.3, 131.0, 128.7, 128.5, 126.6, 125.8, 123.1, 121.3, 113.5, 56.8. HRESIMS *m/z* calcd for $C_{16}H_{13}N_2O_3^+$ 281.0921 $[M+H]^+$, found 281.0926.

*4.1.1.4. 2-(4-fluorobenzoyl)quinazolin-4(3H)-one (**3d**).* White solid, 2.78 g, yield 71%; ^{1}H NMR (600 MHz, DMSO-d_6, *J* in Hz) δ_H 12.65 (s, 1H), 8.28–8.23 (m, 2H), 8.18 (dd, *J* = 7.9, 1.6 Hz, 1H), 7.89–7.83 (m, 1H), 7.75 (d, *J* = 8.1 Hz, 1H), 7.63 (t, *J* = 7.5 Hz, 1H), 7.40 (t, *J* = 8.8 Hz, 2H). ^{13}C NMR (125 MHz, DMSO-d_6) δ_C 186.0, 166.1 (d, $^1J_{C-F}$ = 252.5 Hz), 164.3, 149.3, 147.5, 135.2, 134.6 (d, $^3J_{C-F}$ = 10 Hz), 131.2 (d, $^4J_{C-F}$ = 2.5 Hz), 129.1, 128.8, 126.5, 123.4, 116.2 (d, $^2J_{C-F}$ = 22.5 Hz). HRESIMS *m/z* calcd for $C_{15}H_{10}FN_2O_2^+$ 269.0721 $[M+H]^+$, found 269.0725.

*4.1.1.5. 2-(4-chlorobenzoyl)quinazolin-4(3H)-one(**3e**).* White solid, 3.21 g, yield 77%; ^{1}H NMR (600 MHz, DMSO-d_6, *J* in Hz) δ_H 12.64 (s, 1H), 8.20–8.15 (m, 3H), 7.86 (ddd, *J* = 8.4, 7.1, 1.5 Hz, 1H), 7.75 (dd, *J* = 8.1, 1.1 Hz, 1H), 7.65–7.61 (m, 3H). ^{13}C NMR (150 MHz, DMSO-d_6) δ_C 186.5, 161.6, 149.1, 147.6, 139.8, 135.3, 133.4, 133.3, 129.3, 129.2, 129.0, 126.6, 123.5. HRESIMS *m/z* calcd for $C_{15}H_{10}ClN_2O_2^+$ 285.0425 $[M+H]^+$, found 285.0432.

*4.1.1.6. 2-(4-(trifluoromethoxy)benzoyl)quinazolin-4(3H)-one (**3f**).* White solid, 1.83 g, yield 37%;^{1}H NMR (600 MHz, DMSO-d_6, *J* in Hz) δ_H 12.65 (s, 1H), 8.32–8.28 (m, 2H), 8.18 (dd, *J* = 7.9, 1.5 Hz, 1H), 7.86 (ddd, *J* = 8.5, 7.1, 1.6 Hz, 1H), 7.76 (dd, *J* = 8.3, 1.2 Hz, 1H), 7.66–7.61 (m, 1H), 7.55–7.52 (m, 2H). ^{13}C NMR (150 MHz, DMSO-d_6) δ_C 186.2, 161.6, 152.7, 149.0, 147.6, 135.3, 134.1, 133.5, 129.3, 129.0, 126.6, 123.5, 120.5 (q, $^1J_{C-F}$ = 255 Hz). HRESIMS *m/z* calcd for $C_{16}H_{10}F_3N_2O_3^+$ 335.0638 $[M+H]^+$, found 335.0643.

*4.1.1.7. 2-(2-(trifluoromethoxy)benzoyl)quinazolin-4(3H)-one (**3g**).* White solid, 1.92 g, yield 39%; ^{1}H NMR (600 MHz, DMSO-d_6, *J* in Hz) δ_H 12.86 (s, 1H), 8.18 (dd, *J* = 7.9, 1.5 Hz, 1H), 7.90 (dd, *J* = 7.7, 1.8 Hz, 1H), 7.82 (ddd, *J* = 8.4, 7.2, 1.6 Hz, 1H), 7.77 (td, *J* = 7.9, 1.8 Hz, 1H), 7.67–7.59 (m, 2H), 7.56 (t, *J* = 7.6 Hz, 1H), 7.52 (d, *J* = 8.4 Hz, 1H). ^{13}C NMR (125 MHz, DMSO-d_6) δ_C 187.4, 161.4, 148.9, 147.5, 146.9, 135.3, 134.8, 132.5, 129.8, 129.5, 128.9, 127.8, 126.6, 123.4, 121.4, 120.3 (q, $^1J_{C-F}$ = 256.25 Hz). HRESIMS *m/z* calcd for $C_{16}H_{10}F_3N_2O_3^+$ 335.0638 $[M+H]^+$, found 335.0646.

*4.1.1.8. 2-(4-(trifluoromethyl)benzoyl)quinazolin-4(3H)-one (**3h**).* White solid, 1.94 g, yield 42%; ^{1}H NMR (600 MHz, DMSO-d_6, *J* in Hz) δ_H 12.68 (s, 1H), 8.32 (d, *J* = 8.1 Hz, 2H), 8.19 (dd, *J* = 8.0, 1.6 Hz, 1H), 7.93 (d, *J* = 8.3 Hz, 2H), 7.86 (ddd, *J* = 8.4, 7.1, 1.5 Hz, 1H), 7.75 (dd, *J* = 8.2, 1.2 Hz, 1H), 7.64 (ddd, *J* = 8.1, 7.1, 1.2 Hz, 1H). ^{13}C NMR (125 MHz, DMSO-d_6) δ_C 186.9, 161.6, 148.7, 147.5, 138.3, 135.4, 133.5 (q, $^2J_{C-F}$ = 27.5 Hz), 132.2, 129.5, 129.1, 126.6, 125.8 (q, $^3J_{C-F}$ = 3.75 Hz), 124.3 (q, $^1J_{C-F}$ = 226.25 Hz), 123.6. HRESIMS *m/z* calcd for $C_{16}H_{10}F_3N_2O_2^+$ 319.0689 $[M+H]^+$, found 319.0695.

*4.1.1.9. 2-(2-(trifluoromethyl)benzoyl)quinazolin-4(3H)-one (**3i**).* White solid, 1.86 g, yield 40%; ^{1}H NMR (600 MHz, DMSO-d_6, *J* in Hz) δ_H 12.84 (s, 1H), 8.18 (dd, *J* = 7.9, 1.6 Hz, 1H), 7.89 (dd, *J* = 6.7, 2.4 Hz, 1H), 7.86–7.83 (m, 1H), 7.82–7.78 (m, 3H), 7.67–7.59 (m, 2H). ^{13}C NMR (125 MHz, DMSO-d_6) δ_C 189.8, 161.3, 148.3, 147.3, 135.6 (q, $^3J_{C-F}$ = 2 Hz), 135.3, 132.5, 131.9, 130.5, 129.9, 129.2, 127.4 (q, $^2J_{C-F}$ = 32.5 Hz), 127.0 (q, $^3J_{C-F}$ = 5 Hz), 126.6, 124.2 (q, $^1J_{C-F}$ = 271.25 Hz), 123.6. HRESIMS *m/z* calcd for $C_{16}H_{10}F_3N_2O_2^+$ 319.0689 $[M+H]^+$, found 319.0695.

*4.1.2. General procedures to synthesize **4a**–**4u***

I_2 (362.25 mg, 1.43 mmol, 1.1 eq) was added to a mixture of **2j** (272.77 mg, 1.3 mmol, 1 eq) and DMSO (3 mL). The solution was stirred at 110 °C, then **1a**–**1u** (1 eq) in 3 mL DMSO was added dropwise to the mixture during 1 h. After the complete disappearance of the starting material, a sodium thiosulfate solution (0.2 g $Na_2S_2O_3$ in 12 mL water) was added dropwise to the reaction system. Filtration and drying, the residue was purified by silica gel chromatography to yield the desired products **4a**–**4u**.

*4.1.2.1. 2-(3,4,5-trimethoxybenzoyl)quinazolin-4(3H)-one (**4a**).* White solid, 293 mg, yield 66%; ^{1}H NMR (400 MHz, DMSO-d_6, *J* in Hz) δ_H 12.65 (s, 1H), 8.22 (dd, *J* = 7.9, 1.5 Hz, 1H), 7.90 (ddd, *J* = 8.5, 7.0, 1.6 Hz, 1H), 7.83 (dd, *J* = 8.3, 1.3 Hz, 1H), 7.66 (ddd, *J* = 8.1, 7.1, 1.3 Hz, 1H), 7.58 (s, 2H), 3.84 (s, 6H), 3.81 (s, 3H). ^{13}C NMR (100 MHz, DMSO-d_6) δ_C 185.9, 161.6, 153.0, 149.4, 147.6, 143.5, 135.2, 129.4, 129.0, 128.9, 126.5, 123.4, 109.2, 60.8, 56.6. HRESIMS *m/z* calcd for $C_{18}H_{15}N_2O_5^-$ 339.0986 $[M-H]^-$, found 339.0984.

*4.1.2.2. 5-Fluoro-2-(3,4,5-trimethoxybenzoyl)quinazolin-4(3H)-one (**4b**).* Yellow solid, 239 mg, yield 51%; ^{1}H NMR (400 MHz, DMSO-d_6, *J* in Hz) δ_H 12.69 (s, 1H), 7.86 (td, *J* = 8.2, 5.5 Hz, 1H), 7.62 (dd, *J* = 8.2, 1.0 Hz, 1H), 7.54 (s, 2H), 7.40 (ddd, *J* = 11.1, 8.2, 1.1 Hz, 1H), 3.83 (s, 6H), 3.81 (s, 3H). ^{13}C NMR (125 MHz, DMSO-d_6) δ_C 185.4, 160.5 (d, $^1J_{C-F}$ = 261.25 Hz), 158.6, 152.6, 149.7 (d, $^2J_{C-F}$ = 68.75 Hz), 143.3, 135.4 (d, $^3J_{C-F}$ = 11.25 Hz), 128.8, 124.4, 114.8 (d, $^2J_{C-F}$ = 20 Hz), 112.3 (d, $^3J_{C-F}$ = 6.25 Hz), 108.7, 60.35, 56.22. HRESIMS *m/z* calcd for $C_{18}H_{14}FN_2O_5^-$ 357.0892 $[M-H]^-$, found 357.0894.

*4.1.2.3. 6-Fluoro-2-(3,4,5-trimethoxybenzoyl)quinazolin-4(3H)-one (**4c**).* White solid, 267 mg, yield 57%; ^{1}H NMR (400 MHz, DMSO-d_6, *J* in Hz) δ_H 12.83 (s, 1H), 8.03 (dd, *J* = 8.0, 1.4 Hz, 1H), 7.78 (ddd, *J* = 10.4, 8.0, 1.4 Hz, 1H), 7.68 (s, 2H), 7.67–7.62 (m, 1H), 3.84 (s, 6H), 3.81 (s, 3H). ^{13}C NMR (150 MHz, DMSO-d_6) δ_C 184.8, 160.5, 157.2 (d, $^1J_{C-F}$ = 253.5 Hz), 152.5, 149.3, 143.2, 136.5, 128.9 (d, $^3J_{C-F}$ = 6 Hz), 128.8, 124.9, 121.8, 120.2 (d, $^2J_{C-F}$ = 18 Hz), 109.0, 60.3, 56.1. HRESIMS *m/z* calcd for $C_{18}H_{14}FN_2O_5^-$ 357.0892 $[M-H]^-$, found 357.0890.

*4.1.2.4. 7-Fluoro-2-(3,4,5-trimethoxybenzoyl)quinazolin-4(3H)-one (**4d**).* White solid, 312 mg, yield 67%; ^{1}H NMR (400 MHz, DMSO-d_6, *J* in Hz) δ_H 12.77 (s, 1H), 8.26 (dd, *J* = 8.8, 6.1 Hz, 1H), 7.64 (dd, *J* = 9.9, 2.5 Hz, 1H), 7.54 (s, 2H), 7.53–7.46 (m, 1H), 3.83 (s, 6H), 3.80 (s, 3H). ^{13}C NMR (100 MHz, DMSO-d_6) δ_C 185.6, 166.0 (d, $^1J_{C-F}$ = 250 Hz), 160.8, 156.6, 152.8, 150.5, 143.4, 129.3 (d, $^3J_{C-F}$ = 9 Hz), 128.9, 120.1, 117.0 (d, $^2J_{C-F}$ = 23 Hz), 113.7 (d, $^2J_{C-F}$ = 21 Hz), 108.9, 60.5, 56.4. HRESIMS *m/z* calcd for $C_{18}H_{16}FN_2O_5^+$ 359.1038 $[M+H]^+$, found 359.1039.

*4.1.2.5. 8-Fluoro-2-(3,4,5-trimethoxybenzoyl)quinazolin-4(3H)-one (**4e**).* Yellow solid, 273 mg, yield 59%; ^{1}H NMR (400 MHz, DMSO-d_6, *J* in Hz) δ_H 12.84 (s, 1H), 8.03 (dd, *J* = 7.9, 1.4 Hz, 1H), 7.84–7.75 (m, 1H), 7.68 (s, 2H), 7.65 (dt, *J* = 8.0, 4.0 Hz, 1H), 3.85 (s, 6H), 3.81 (s, 3H). ^{13}C NMR (150 MHz, DMSO-d_6) δ_C 184.8, 160.4, 157.2 (d, $^1J_{C-F}$ = 253.5 Hz), 152.5, 152.5, 149.2, 143.2, 136.5 (d, $^2J_{C-F}$ = 19.5 Hz), 129.0 (d, $^3J_{C-F}$ = 9 Hz), 128.8, 124.9, 121.8 (d, $^4J_{C-F}$ = 4.5 Hz), 120.2 (d,

$^2J_{C\text{-}F}$ = 12 Hz), 109.0, 60.3, 56.1. HRESIMS *m/z* calcd for $C_{18}H_{14}FN_2O_5^-$ 357.0892 $[M-H]^-$, found 357.0890.

*4.1.2.6. 6,7-Difluoro-2-(3,4,5-trimethoxybenzoyl)quinazolin-4(3H)-one (**4f**).* White solid, 277 mg, yield 57%; ^{1}H NMR (400 MHz, DMSO-d_6, *J* in Hz) δ_H 12.91 (s, 1H), 8.13 (dd, *J* = 10.3, 8.6 Hz, 1H), 7.97 (dd, *J* = 11.2, 7.3 Hz, 1H), 7.53 (s, 2H), 3.84 (s, 6H), 3.80 (s, 3H). ^{13}C NMR (150 MHz, DMSO-d_6) δ_C 185.3, 160.1, 154.0 (dd, $^1J_{C\text{-}F}$ = 253.5 Hz, $^1J_{C\text{-}F}$ = 15 Hz), 152.6, 149.9, 149.6 (dd, $^1J_{C\text{-}F}$ = 249 Hz, $^1J_{C\text{-}F}$ = 13.5 Hz), 145.3 (d, $^3J_{C\text{-}F}$ = 10.5 Hz), 143.3, 128.7, 120.5 (d, $^3J_{C\text{-}F}$ = 6 Hz), 116.5 (d, $^2J_{C\text{-}F}$ = 18 Hz), 113.7 (d, $^2J_{C\text{-}F}$ = 18 Hz), 108.8, 60.4, 56.2. HRESIMS *m/z* calcd for $C_{18}H_{15}F_2N_2O_5^+$ 377.0944 $[M+H]^+$, found 377.0940.

*4.1.2.7. 5-Chloro-2-(3,4,5-trimethoxybenzoyl)quinazolin-4(3H)-one (**4g**).* White solid, 241 mg, yield 50%; ^{1}H NMR (400 MHz, DMSO-d_6, *J* in Hz) δ_H 12.68 (s, 1H), 7.82–7.71 (m, 2H), 7.64 (dd, *J* = 7.6, 1.4 Hz, 1H), 7.55 (s, 2H), 3.83 (s, 6H), 3.81 (s, 3H). ^{13}C NMR (100 MHz, DMSO-d_6) δ_C 185.4, 159.6, 152.7, 150.0, 149.9, 143.4, 134.7, 132.8, 130.8, 128.9, 128.0, 120.1, 108.8, 60.5, 56.4. HRESIMS *m/z* calcd for $C_{18}H_{16}ClN_2O_5^+$ 375.0742 $[M+H]^+$, found 375.0741.

*4.1.2.8. 6-Chloro-2-(3,4,5-trimethoxybenzoyl)quinazolin-4(3H)-one (**4h**).* White solid, 312 mg, yield 64%; ^{1}H NMR (400 MHz, DMSO-d_6, *J* in Hz) δ_H 12.86 (s, 1H), 8.15 (d, *J* = 2.5 Hz, 1H), 7.93 (dd, *J* = 8.7, 2.5 Hz, 1H), 7.85 (d, *J* = 8.7 Hz, 1H), 7.55 (s, 2H), 3.84 (s, 6H), 3.81 (s, 3H). ^{13}C NMR (100 MHz, DMSO-d_6) δ_C 185.6, 160.5, 152.7, 149.6, 146.1, 143.3, 135.0, 133.0, 130.8, 129.0, 125.2, 124.4, 108.9, 60.5, 56.3. HRESIMS *m/z* calcd for $C_{18}H_{16}ClN_2O_5^+$ 375.0742 $[M+H]^+$, found 375.0741.

*4.1.2.9. 7-Chloro-2-(3,4,5-trimethoxybenzoyl)quinazolin-4(3H)-one (**4i**).* White solid, 304 mg, yield 63%; ^{1}H NMR (400 MHz, DMSO-d_6, *J* in Hz) δ_H 12.83 (s, 1H), 8.20 (d, *J* = 8.5 Hz, 1H), 7.90 (s, 1H), 7.68 (s, 1H), 7.53 (s, 2H), 3.84 (s, 6H), 3.81 (s, 3H). ^{13}C NMR (150 MHz, DMSO-d_6) δ_C 185.5, 152.6, 150.4, 148.4, 143.3, 139.3, 128.7, 128.6, 128.0, 127.5, 121.8, 108.8, 60.3, 56.2. HRESIMS *m/z* calcd for $C_{18}H_{16}ClN_2O_5^+$ 375.0742 $[M+H]^+$, found 375.0740.

*4.1.2.10. 8-Chloro-2-(3,4,5-trimethoxybenzoyl)quinazolin-4(3H)-one (**4j**).* White solid, 212 mg, yield 44%; ^{1}H NMR (400 MHz, DMSO-d_6, *J* in Hz) δ_H 12.84 (s, 1H), 8.18 (dd, *J* = 8.0, 1.4 Hz, 1H), 8.07 (dd, *J* = 7.8, 1.4 Hz, 1H), 7.77 (s, 2H), 7.64 (t, *J* = 7.9 Hz, 1H), 3.87 (s, 6H), 3.82 (s, 3H). ^{13}C NMR (125 MHz, DMSO-d_6) δ_C 184.2, 160.8, 152.4, 149.0, 143.9, 143.2, 134.8, 132.0, 129.0, 128.7, 125.2, 124.8, 109.1, 60.3, 56.1. HRESIMS *m/z* calcd for $C_{18}H_{14}ClN_2O_5^-$ 373.0597 $[M-H]^-$, found 373.0595.

*4.1.2.11. 5-Bromo-2-(3,4,5-trimethoxybenzoyl)quinazolin-4(3H)-one (**4k**).* Yellow solid, 344 mg, yield 63%; ^{1}H NMR (400 MHz, DMSO-d_6, *J* in Hz) δ_H 12.70 (s, 1H), 7.85 (dd, *J* = 7.7, 1.3 Hz, 1H), 7.78 (dd, *J* = 8.1, 1.3 Hz, 1H), 7.69 (t, *J* = 7.9 Hz, 1H), 7.55 (s, 2H), 3.83 (s, 6H), 3.81 (s, 3H). ^{13}C NMR (150 MHz, pyridine-d_5) δ_C 186.2, 161.1, 153.8, 150.9, 150.1, 144.9, 135.6, 134.9, 130.3, 129.5, 123.5, 122.6, 122.1, 110.4, 61.1, 56.7. HRESIMS *m/z* calcd for $C_{18}H_{16}BrN_2O_5^+$ 419.0237 $[M+H]^+$, found 419.0235.

*4.1.2.12. 6-Bromo-2-(3,4,5-trimethoxybenzoyl)quinazolin-4(3H)-one (**4l**).* Yellow solid, 266 mg, yield 49%; ^{1}H NMR (400 MHz, DMSO-d_6, *J* in Hz) δ_H 12.86 (s, 1H), 8.29 (d, *J* = 2.4 Hz, 1H), 8.04 (dd, *J* = 8.6, 2.4 Hz, 1H), 7.77 (d, *J* = 8.7 Hz, 1H), 7.55 (s, 2H), 3.83 (s, 6H), 3.81 (s, 3H). ^{13}C NMR (100 MHz, DMSO-d_6) δ_C 185.5, 160.3, 152.7, 149.7, 146.4, 143.3, 137.7, 130.8, 128.9, 128.3, 124.7, 121.3, 108.9, 60.5, 56.3. HRESIMS *m/z* calcd for $C_{18}H_{16}BrN_2O_5^+$ 419.0237 $[M+H]^+$, found 419.0234.

*4.1.2.13. 7-Bromo-2-(3,4,5-trimethoxybenzoyl)quinazolin-4(3H)-one (**4 m**).* Yellow solid, 409 mg, yield 75%; ^{1}H NMR (400 MHz, DMSO-d_6, *J* in Hz) δ_H 12.83 (s, 1H), 8.12 (d, *J* = 8.5 Hz, 1H), 8.05 (d, *J* = 1.9 Hz, 1H), 7.81 (dd, *J* = 8.5, 1.9 Hz, 1H), 7.53 (s, 2H), 3.84 (s, 6H), 3.81 (s, 3H). ^{13}C NMR (150 MHz, DMSO-d_6) δ_C 185.7, 161.1, 152.8, 150.6, 148.7, 143.4, 131.5, 130.7, 128.9, 128.4, 128.2, 122.3, 108.9, 60.5, 56.4. HRESIMS *m/z* calcd for $C_{18}H_{16}BrN_2O_5^+$ 419.0237 $[M+H]^+$, found 419.0234.

*4.1.2.14. 8-Bromo-2-(3,4,5-trimethoxybenzoyl)quinazolin-4(3H)-one (**4n**).* White solid, 245 mg, yield 45%; ^{1}H NMR (400 MHz, DMSO-d_6, *J* in Hz) δ_H 12.84 (s, 1H), 8.22 (t, *J* = 6.5 Hz, 2H), 7.74 (s, 2H), 7.56 (t, *J* = 8.0 Hz, 1H), 3.88 (s, 6H), 3.82 (s, 3H). ^{13}C NMR (150 MHz, pyridine-d_5) δ_C 185.6, 162.4, 153.8, 146.4, 144.9, 138.7, 135.5, 130.3, 129.8, 126.8, 126.4, 124.8, 123.5, 110.8, 61.1, 56.8. HRESIMS *m/z* calcd for $C_{18}H_{16}BrN_2O_5^+$ 419.0237 $[M+H]^+$, found 419.0237.

*4.1.2.15. 6-Nitro-2-(3,4,5-trimethoxybenzoyl)quinazolin-4(3H)-one (**4o**).* Yellow solid, 273 mg, yield 55%; ^{1}H NMR (400 MHz, DMSO-d_6, *J* in Hz) δ_H 8.87 (d, *J* = 2.7 Hz, 1H), 8.59 (dd, *J* = 8.9, 2.7 Hz, 1H), 8.00 (d, *J* = 9.0 Hz, 1H), 7.52 (s, 2H), 3.83 (s, 6H), 3.81 (s, 3H). ^{13}C NMR (150 MHz, DMSO-d_6) δ_C 185.6, 160.8, 152.7, 152.3, 146.0, 143.5, 130.1, 128.62, 128.55, 123.3, 121.9, 108.8, 60.4, 56.3. HRESIMS *m/z* calcd for $C_{18}H_{14}N_3O_7^-$ 384.0837 $[M-H]^-$, found 384.0836.

*4.1.2.16. 7-Nitro-2-(3,4,5-trimethoxybenzoyl)quinazolin-4(3H)-one (**4p**).* Yellow solid, 254 mg, yield 51%; ^{1}H NMR (400 MHz, DMSO-d_6, *J* in Hz) δ_H 13.12 (s, 1H), 8.51 (d, *J* = 2.2 Hz, 1H), 8.43 (d, *J* = 8.6 Hz, 1H), 8.34 (dd, *J* = 8.7, 2.2 Hz, 1H), 7.53 (s, 2H), 3.83 (overlapped, 9H). ^{13}C NMR (150 MHz, DMSO-d_6) δ_C 185.8, 160.7, 152.8, 151.5, 148.0, 143.5, 128.8, 128.4, 127.5, 123.3, 122.0, 108.9, 60.5, 56.4. HRESIMS *m/z* calcd for $C_{18}H_{14}N_3O_7^-$ 384.0837 $[M-H]^-$, found 384.0839.

*4.1.2.17. 5-Methoxy-2-(3,4,5-trimethoxybenzoyl)quinazolin-4(3H)-one (**4q**).* White solid, 173 mg, yield 36%; ^{1}H NMR (400 MHz, DMSO-d_6, *J* in Hz) δ_H 12.26 (s, 1H), 7.76 (t, *J* = 8.1 Hz, 1H), 7.55 (s, 2H), 7.32 (d, *J* = 8.0 Hz, 1H), 7.16 (d, *J* = 8.3 Hz, 1H), 3.90 (s, 3H), 3.83 (s, 6H), 3.80 (s, 3H). ^{13}C NMR (100 MHz, DMSO-d_6) δ_C 185.2, 159.8, 159.1, 152.5, 149.7, 149.3, 147.2, 143.1, 135.0, 133.8, 128.8, 120.1, 112.2, 110.2, 108.6, 60.3, 56.2, 56.1. HRESIMS *m/z* calcd for $C_{19}H_{19}N_2O_6^+$ 371.1238 $[M+H]^+$, found 371.1234.

*4.1.2.18. 6-Methoxy-2-(3,4,5-trimethoxybenzoyl)quinazolin-4(3H)-one (**4r**).* White solid, 227 mg, yield 47%; ^{1}H NMR (400 MHz, DMSO-d_6, *J* in Hz) δ_H 12.55 (s, 1H), 7.80 (d, *J* = 8.9 Hz, 1H), 7.61 (s, 1H), 7.60 (s, 2H), 7.50 (dd, *J* = 9.0, 3.0 Hz, 1H), 3.92 (s, 3H), 3.84 (s, 6H), 3.80 (s, 3H). ^{13}C NMR (100 MHz, DMSO-d_6) δ_C 185.1, 160.9, 159.4, 153.8, 152.4, 146.7, 142.9, 141.3, 130.4, 129.2, 124.1, 108.8, 106.3, 60.3, 56.1, 55.9. HRESIMS *m/z* calcd for $C_{19}H_{19}N_2O_6^+$ 371.1238 $[M+H]^+$, found 371.1235.

*4.1.2.19. 7-Methoxy-2-(3,4,5-trimethoxybenzoyl)quinazolin-4(3H)-one (**4s**).* White solid, 351 mg, yield 73%; ^{1}H NMR (400 MHz, DMSO-d_6, *J* in Hz) δ_H 12.53 (s, 1H), 8.11 (d, *J* = 8.8 Hz, 1H), 7.52 (s, 2H), 7.31–7.14 (m, 2H), 3.91 (s, 3H), 3.84 (s, 6H), 3.81 (s, 3H). ^{13}C NMR (150 MHz, DMSO-d_6) δ_C 185.7, 164.3, 160.7, 152.6, 149.7, 149.5, 143.1, 129.0, 127.6, 117.7, 116.2, 109.7, 108.7, 60.3, 56.2, 55.9. HRESIMS *m/z* calcd for $C_{19}H_{17}N_2O_6^-$ 369.1092 $[M-H]^-$, found 369.1089.

*4.1.2.20. 8-Methoxy-2-(3,4,5-trimethoxybenzoyl)quinazolin-4(3H)-one (**4t**).* White solid, 31 mg, yield 6%; ^{1}H NMR (400 MHz, $CDCl_3$, *J* in Hz) δ_H 10.32 (s, 1H), 8.25 (s, 2H), 7.95 (dd, *J* = 7.9, 1.2 Hz, 1H), 7.58 (t, *J* = 8.1 Hz, 1H), 7.29 (dd, *J* = 8.2, 1.2 Hz, 1H), 4.00 (overlapped, 12H). ^{13}C NMR (150 MHz, DMSO-d_6) δ_C 185.3, 159.8, 159.2, 152.5, 149.7, 149.3, 143.2, 135.1, 128.9, 120.1, 112.3, 110.3, 108.7, 60.3, 56.2,

56.2. HRESIMS *m/z* calcd for $C_{19}H_{17}N_2O_6^-$ 369.1092 $[M-H]^-$, found 369.1090.

*4.1.2.21. 6,7-Dimethoxy-2-(3,4,5-trimethoxybenzoyl)quinazolin-4(3H)-one (**4u**).* White solid, 106 mg, yield 20%; ^{1}H NMR (400 MHz, $CDCl_3$, *J* in Hz) δ_H 10.37 (s, 1H), 7.83 (s, 2H), 7.70 (s, 1H), 7.22 (s, 1H), 4.03 (s, 3H), 4.01 (s, 3H), 3.97 (s, 3H), 3.94 (s, 6H). ^{13}C NMR (100 MHz, $CDCl_3$) δ_C 183.8, 160.3, 155.2, 152.7, 151.1, 145.2, 143.9, 143.4, 128.8, 117.1, 109.5, 109.3, 105.8, 61.0, 56.5, 56.4, 56.3. HRESIMS *m/z* calcd for $C_{20}H_{21}N_2O_7^+$ 401.1343 $[M+H]^+$, found 401.1341.

*4.1.3. General procedures to synthesize **5a**–**5c***

The compound **4a** (80 mg, 235.07 μmol, 1 eq) was added to a stirred solution of DMF (4 mL). After compound **4a** was dissolved, K_2CO_3 (49 mg, 352.6 μmol, 1.5 eq) and appropriate halogenated compound (2 eq) were added to the solvent. The reaction mixture was heated to 80 °C. After the reaction was complete (monitored by TLC), the solvent was removed under reduced pressure, the solid was filtered and washed with acetone then with water to yield the pure products.

*4.1.3.1. 3-Methyl-2-(3,4,5-trimethoxybenzoyl)quinazolin-4(3H)-one (**5a**).* White solid, 11 mg, yield 13%; ^{1}H NMR (400 MHz, DMSO-d_6, *J* in Hz) δ_H 8.24 (dd, *J* = 8.0, 1.6 Hz, 1H), 7.87 (ddd, *J* = 8.5, 7.1, 1.6 Hz, 1H), 7.71 (dd, *J* = 8.3, 1.2 Hz, 1H), 7.64 (ddd, *J* = 8.2, 7.1, 1.2 Hz, 1H), 7.38 (s, 2H), 3.814 (s, 6H), 3.808 (s, 3H), 3.41 (s, 3H). ^{13}C NMR (100 MHz, DMSO-d_6) δ_C 187.4, 161.4, 153.5, 152.1, 146.7, 144.4, 135.1, 129.1, 128.5, 127.9, 126.7, 122.0, 108.7, 60.8, 56.8, 32.2. HRESIMS *m/z* calcd for $C_{19}H_{19}N_2O_5^+$ 355.1288 $[M+H]^+$, found 355.1282.

*4.1.3.2. 3-Allyl-2-(3,4,5-trimethoxybenzoyl)quinazolin-4(3H)-one (**5b**).* White solid, 15 mg, yield 17%; ^{1}H NMR (400 MHz, $CDCl_3$, *J* in Hz) δ_H 8.38 (dd, *J* = 7.9, 1.5 Hz, 1H), 7.84–7.72 (m, 2H), 7.59 (ddd, *J* = 8.2, 7.0, 1.4 Hz, 1H), 7.27 (s, 2H), 5.88 (ddt, *J* = 16.5, 10.7, 5.9 Hz, 1H), 5.18–5.10 (m, 2H), 4.75 (dt, *J* = 5.9, 1.4 Hz, 2H), 3.96 (s, 3H), 3.86 (s, 6H). ^{13}C NMR (100 MHz, $CDCl_3$) δ_C 186.6, 161.3, 153.4, 151.0, 146.4, 144.7, 134.9, 131.7, 129.1, 128.4, 128.0, 127.3, 122.1, 119.6, 108.5, 61.2, 56.6, 46.6. HRESIMS *m/z* calcd for $C_{21}H_{21}N_2O_5^+$ 381.1445 $[M+H]^+$, found 381.1440.

*4.1.3.3. 3-(Prop-2-yn-1-yl)-2-(3,4,5-trimethoxybenzoyl)quinazolin-4(3H)-one (**5c**).* White solid, 8 mg, yield 9%; ^{1}H NMR (400 MHz, $CDCl_3$, *J* in Hz) δ_H 8.39 (dd, *J* = 8.0, 1.6 Hz, 1H), 7.83–7.74 (m, 1H), 7.75 (d, *J* = 8.5 Hz, 1H), 7.60 (ddd, *J* = 7.5, 6.8, 1.3 Hz, 1H), 7.36 (s, 2H), 5.08 (d, *J* = 2.5 Hz, 2H), 3.97 (s, 3H), 3.87 (s, 6H), 2.11 (t, *J* = 2.5 Hz, 1H). ^{13}C NMR (100 MHz, $CDCl_3$) δ_C 186.3, 160.6, 153.0, 149.8, 145.9, 144.3, 135.0, 129.0, 128.6, 128.1, 127.3, 121.7, 108.6, 78.1, 73.6, 61.1, 56.4, 32.7. HRESIMS *m/z* calcd for $C_{21}H_{19}N_2O_5^+$ 379.1288 $[M+H]^+$, found 379.1285.

*4.1.4. General procedures to synthesize **6a**–**6b***

To a room temperature solution of compound **4a** (100 mg, 293.83 μmol, 1eq) and BOP (169 mg, 381.98 μmol, 1.3 eq) in MeCN (4 mL) were added DBU (67 mg, 440.75 μmol, 1.5 eq). Then appropriate alcohol (4 mL) was added to the vial. The reaction mixture was stirred at 85 °C for 2 days. After the reaction was complete (monitored by TLC), the solvent was removed under reduced pressure, the solid was filtered and washed with dimethyl sulfoxide then with water to yield the pure product.

*4.1.4.1. (4-Ethoxyquinazolin-2-yl) (3,4,5-trimethoxyphenyl)methanone (**6a**).* White solid, 54 mg, yield 50%; ^{1}H NMR (400 MHz, $CDCl_3$, *J* in Hz) δ_H 8.26 (dd, *J* = 8.3, 1.6 Hz, 1H), 8.05 (dd, *J* = 8.4, 1.5 Hz, 1H), 7.89 (ddd, *J* = 8.4, 6.9, 1.5 Hz, 1H), 7.66 (ddd, *J* = 8.3, 7.0, 1.4 Hz, 1H), 7.44 (s, 2H), 4.71 (q, *J* = 7.1, 2H), 3.94 (s, 3H), 3.86 (s, 6H), 1.52 (td, *J* = 7.1, 1.6 Hz, 3H). ^{13}C NMR (100 MHz, $CDCl_3$) δ_C 190.5, 167.4, 158.4, 152.8, 150.4, 143.2, 134.1, 130.3, 128.5, 128.3, 123.7, 116.5, 108.7, 63.7, 60.9, 56.3, 14.3. HRESIMS *m/z* calcd for $C_{20}H_{21}N_2O_5^+$ 369.1445 $[M+H]^+$, found 369.1440.

*4.1.4.2. (4-Isopropoxyquinazolin-2-yl) (3,4,5-trimethoxyphenyl) methanone (**6b**).* White solid, 21 mg, yield 19%; ^{1}H NMR (400 MHz, $CDCl_3$, *J* in Hz) δ_H 8.41 (t, *J* = 6.8 Hz, 1H), 8.01 (d, *J* = 5.7 Hz, 2H), 7.94–7.83 (m, 2H), 7.69–7.65 (m, 1H), 3.99 (overlapped, 10H), 1.26 (overlapped, 6H). ^{13}C NMR (150 MHz, $CDCl_3$) δ_C 183.3, 160.7, 152.7, 147.4, 146.1, 144.1, 134.9, 129.5, 129.2, 128.5, 126.9, 123.2, 109.6, 61.0, 56.3, 31.2, 29.6. HRESIMS *m/z* calcd for $C_{21}H_{23}N_2O_5^+$ 383.1601 $[M+H]^+$, found 383.1595.

*4.1.5. General procedures to synthesize **8a**–**8d***

K_2CO_3 (49 mg, 352.6 μmol, 1.5 eq) was added to a stirred solution of compound **4a** (80 mg, 235.07 μmol, 1 eq) and **7a**–**7d** (1.5 eq) in DMF (4 mL). The reaction mixture was heated to 80 °C for 12 h. The mixture was cooled, separated by filtration and purified by chromatography on silica gel using CH_2Cl_2 to obtain **8a**–**8d**.

*4.1.5.1. 3-((5-(4-chlorophenyl)-1,3,4-oxadiazol-2-yl)methyl)-2-(3,4,5-trimethoxybenz- oyl)quinazolin-4(3H)-one (**8a**).* White solid, 21 mg, yield 18%; ^{1}H NMR (400 MHz, $CDCl_3$, *J* in Hz) δ_H 8.39 (dd, *J* = 8.0, 1.5 Hz, 1H), 7.88–7.78 (m, 4H), 7.63 (ddd, *J* = 8.2, 6.9, 1.4 Hz, 1H), 7.44–7.40 (m, 2H), 7.37 (s, 2H), 5.78 (s, 2H), 3.93 (s, 3H), 3.85 (s, 6H). ^{13}C NMR (100 MHz, $CDCl_3$) δ_C 186.7, 164.6, 161.9, 161.0, 153.0, 149.6, 145.9, 144.5, 138.4, 135.3, 129.4, 129.0, 128.6, 128.3, 128.2, 127.4, 121.7, 121.6, 108.8, 61.1, 56.4, 38.0. HRESIMS *m/z* calcd for $C_{27}H_{22}ClN_4O_6^+$ 533.1222 $[M+H]^+$, found 533.1219.

*4.1.5.2. 3-((5-(4-fluorophenyl)-1,3,4-oxadiazol-2-yl)methyl)-2-(3,4,5-trimethoxybenz- oyl)quinazolin-4(3H)-one (**8b**).* White solid, 13 mg, yield 11%; ^{1}H NMR (400 MHz, $CDCl_3$, *J* in Hz) δ_H 8.40 (dd, *J* = 8.0, 1.5 Hz, 1H), 7.92–7.77 (m, 4H), 7.64 (ddd, *J* = 8.2, 6.9, 1.4 Hz, 1H), 7.37 (s, 2H), 7.13 (t, *J* = 8.7 Hz, 2H), 5.79 (s, 2H), 3.93 (s, 3H), 3.85 (s, 6H). ^{13}C NMR (100 MHz, $CDCl_3$) δ_C 186.8, 165.10 (d, $^1J_{C\text{-}F}$ = 252 Hz), 164.7, 161.9, 161.1, 153.2, 149.7, 146.0, 144.7, 135.4, 129.4 (d, $^3J_{C\text{-}F}$ = 8.1 Hz), 129.1, 128.7, 128.4, 127.6, 121.7, 119.7 (d, $^4J_{C\text{-}F}$ = 3 Hz), 116.6 (d, $^2J_{C\text{-}F}$ = 22 Hz), 116.4, 109.0, 61.2, 56.5, 38.0. HRESIMS *m/z* calcd for $C_{27}H_{22}FN_4O_6^+$ 517.1518 $[M+H]^+$, found 517.1513.

*4.1.5.3. 3-((5-(p-tolyl)-1,3,4-oxadiazol-2-yl)methyl)-2-(3,4,5-trimethoxybenzoyl)quin-azolin-4(3H)-one (**8c**).* White solid, 17 mg, yield 15%; ^{1}H NMR (400 MHz, $CDCl_3$, *J* in Hz) δ_H 8.40 (dd, *J* = 7.9, 1.4 Hz, 1H), 7.87–7.71 (m, 4H), 7.67–7.59 (m, 1H), 7.36 (d, *J* = 1.1 Hz, 2H), 7.23 (d, *J* = 7.9 Hz, 2H), 5.80 (s, 2H), 3.91 (s, 3H), 3.84 (s, 6H), 2.39 (s, 3H). ^{13}C NMR (100 MHz, $CDCl_3$) δ_C 186.7, 165.6, 161.4, 161.0, 153.0, 149.7, 145.9, 144.5, 142.6, 135.2, 129.7, 128.9, 128.6, 128.2, 127.4, 126.9, 121.6, 120.4, 108.8, 61.0, 56.4, 37.8, 21.6. HRESIMS *m/z* calcd for $C_{28}H_{25}N_4O_6^+$ 513.1769 $[M+H]^+$, found 513.1769.

*4.1.5.4. 3-((5-(furan-2-yl)-1,3,4-oxadiazol-2-yl)methyl)-2-(3,4,5-trimethoxybenzoyl)q-uinazolin-4(3H)-one (**8d**).* White solid, 31 mg, yield 27%; ^{1}H NMR (400 MHz, $CDCl_3$, *J* in Hz) δ_H 8.40 (dd, *J* = 7.9, 1.5 Hz, 1H), 7.88–7.77 (m, 2H), 7.68–7.54 (m, 2H), 7.36 (s, 2H), 7.05 (dd, *J* = 3.5, 0.8 Hz, 1H), 6.55 (dd, *J* = 3.5, 1.8 Hz, 1H), 5.78 (s, 2H), 3.93 (s, 3H), 3.86 (s, 6H). ^{13}C NMR (100 MHz, $CDCl_3$) δ_C 186.7, 161.0, 160.9, 158.1, 153.0, 149.6, 145.9, 144.4, 138.7, 135.2, 128.9, 128.5, 128.3, 127.4, 121.6, 114.6, 112.2, 108.8, 61.0, 56.4, 37.8. HRESIMS *m/z* calcd for $C_{25}H_{21}N_4O_7^+$ 489.1405 $[M+H]^+$, found 489.1399.

*4.1.6. Preparation of target compound **9***

Compound **4a** (80 mg, 235.07 μmol, 1 eq) was added to phosphorus oxychloride (0.5 mL). The reaction mixture was heated to 100 °C for 1 h. The mixture was cooled, the solvent was removed under reduced pressure, and the solid was filtered and washed with dimethyl sulfoxide then with water to yield the pure product.

*4.1.6.1. (4-Quinazolin-2-yl) (3,4,5-trimethoxyphenyl)methanone (**9**).* White solid, 72 mg, yield 85%; ^{1}H NMR (400 MHz, DMSO-d_6, J in Hz) δ_H 8.21 (dd, J = 8.0, 1.4 Hz, 1H), 7.89 (ddd, J = 8.5, 7.0, 1.5 Hz, 1H), 7.82 (dd, J = 8.3, 1.2 Hz, 1H), 7.65 (ddd, J = 8.2, 7.1, 1.3 Hz, 1H), 7.57 (s, 2H), 3.83 (s, 6H), 3.80 (s, 3H). ^{13}C NMR (100 MHz, DMSO-d_6) δ_C 185.9, 161.6, 153.0, 149.4, 147.6, 143.5, 135.3, 129.4, 129.0, 128.8, 126.5, 123.3, 109.2, 60.8, 56.6. HRESIMS *m/z* calcd for $C_{18}H_{16}ClN_2O_4^+$ 359.0793 $[M+H]^+$, found 359.0790.

4.2. Materials for biological studies

Roswell Park Memorial Institute (RPMI) 1640, Dulbecco's modified Eagle's medium (DMEM) and Fetal bovine serum (FBS) were purchased from Gibco company. 6-well plates and 96-well plates were purchased from Costar company. HepG2/Bel-7402 (human hepatic carcinoma), A549 (human lung carcinoma), U251 (human glioma carcinoma), NCI−H1299 (human lung carcinoma), HCT116 (human colon carcinoma) cell strains were purchased from EnoGene company.

4.2.1. Cell proliferation assay

All compounds were dissolved in DMSO. HepG2, Bel-7402, A549, U251, NCI−H1299, and HCT116 were seeded into 96-well plates (3×10^3 per well). The cells were cultured overnight in DMEM containing 10% FBS, and then negative control (0.1% DMSO) and different concentrations of compounds were added respectively, and then incubated at 37 °C for 72 h. The antiproliferative effects of the compounds were tested by the MTT assay. The 10% MTT (5 mg/mL, PBS) reagent was added to the medium and the cells were incubated at 37 °C for another 4 h. Then, supernatant was discarded, 100 μL of DMSO was added, and incubated at 37 °C for 10 min. Then the absorbance of the cells was measured at 570 nm. Through MTT measurement, the growth inhibition rate of the compound is calculated as (Ac−As)/(Ac−Ab) × 100% (Ac, absorbance of control wells; As, absorbance of sample wells; Ab, Absorbance of blank wells). The IC_{50} calculator was used to calculate the IC_{50} value corresponding to the concentration that caused 50% inhibition of cell proliferation.

4.2.2. Colony formation assay

HepG2 and Bel-7402 cells were seeded in a 6-well plate at 1000 cells/well. The cells were cultured overnight in DMEM containing 10% FBS. Compound **4a** was added according to the concentration gradient, and the cells were placed in 37 °C cell incubator containing 5% CO_2 for 10 days. Then, the cells were fixed with 4% paraformaldehyde for 15 min, stained with crystal violet for 30 min. Then, the pictures were taken and colony numbers were counted. The clone formation rate relative to the solvent control group was calculated.

4.2.3. Cell cycle arrest analysis

HepG2 and Bel-7402 cells were treated with different concentrations of compound **4a** or DMSO for 48 h. Then, a Cell Cycle and Apoptosis Analysis Kit (Yeasen Biotech Co., Ltd.) was used to determine the phase of the cell cycle by flow cytometry on an FC500 cytometer (Beckman Coulter).

4.2.4. Western blot analysis

The cells were washed with pre-chilled PBS and then resuspended in cell lysis buffer to prepare HepG2 and Bel-7402 cell extracts. The cell lysate was separated on a 12.5% SDS-PAGE gel. After the separation process, the protein was transferred to the PVDF membrane (#IPVH00010, Merck Millipore) and incubated with the antibodies of interest at 4 °C overnight. Cleaved caspases-3 (1:1000, #CST9661, Cell Signaling Technology), cleaved PARP (1:1000, #CST5625, Cell Signaling Technology), Tubulin (1:1000, #CST2148, Cell Signaling Technology), AKT (1:1000, #CST9272, Cell Signaling Technology), P-AKT (1:1000, #CST4060S, Cell Signaling Technology), ERK1/2 (1:1000, #CST4695, Cell signaling Technology), P-ERK1/2 (1:1000, #CST4370S, Cell Signaling Technology). Then, the membranes were washed and incubated with horseradish peroxidase (HRP) conjugated anti-rabbit or anti-mouse secondary antibodies for 1 h. A chemiluminescence imaging system was used to capture protein bands.

4.2.5. Cell apoptosis analysis

HepG2 and Bel-7402 cells were treated with different concentrations of compound **4a** or DMSO for 48 h. Muse™ Annexin V & Dead Cell assay kit (Muse TM Cell Analyzer, Millipore (catalog no. MCH100105)) was used to determine the cell apoptosis by the Muse cell analyzer.

4.2.6. Hoechst 33342 stain

The cells were seeded on a 6-well cell culture plate and the negative control DMSO and different concentrations of compound **4a** were added, then the cells were placed in a 37 °C cell incubator for 48 h. The cells were incubated with 10 μg/mL Hoechst 33342 dye (Beyotime Biotechnology, China) in darkness at 37 °C for 30 min and observed under a fluorescent microscopy.

4.2.7. Intracellular ROS measurement

The cells were incubated with different concentrations of compound **4a** for 48 h. Then, the cells were washed and treated with 10 mM DCFH-DA (Beyotime Biotechnology, China) at 37 °C for 20 min in the dark. The fluorescence was checked with a fluorescent microscopy.

4.2.8. Tumor nude mice model

Female BALB/c nude mice (14−17 g) were inoculated with HepG2 cells (1×10^6 per mouse). When the tumor volume reached 100−200 mm^3, the mice were randomly divided into three groups. Taking injection of (15% *N*-methylpyrrolidone, 25% Solutol HS-15, 60% saline) as the solvent control group, the compound **4a** was dissolved at 4 mg/kg and 8 mg/kg and injected into mice intraperitoneally every day for 20 days. Use a vernier caliper to measure the tumor size and use the following formula to calculate the tumor volume (TV): TV (mm^3) = width^2 × (length/2). The inhibition rates of tumor growth (IRT) were calculated as follows: IRT = 100% × [(M1−M0)−(M2−M0)]/(M1−M0) (M0: Tumor volumes before administration; M1: Tumor volumes in the control group; M2: Tumor volumes in the drug treatment group).

Declaration of competing interest

The authors declare that they have no known competing financial interests or personal relationships that could have appeared to influence the work reported in this paper.

Acknowledgments

We thank Prof. Yu-Cheng Gu at Syngenta Jealott's Hill International Research Centre for his proofreading of the manuscript. This

work was supported by the Program of National Natural Science Foundation of China (Nos. U1706210, 81871868, 41776141, and 41322037), the Program of Natural Science Foundation of Shandong Province of China (No. JQ201510), the Fundamental Research Funds for the Central Universities (Nos. 201841004 and 202042011), the Marine S&T Fund of Shandong Province for Pilot National Laboratory for Marine Science and Technology (Qingdao) (Nos. 2018SDKJ0403-2 and 2015ASKJ02), the Taishan Scholars Program, China (No. tsqn20161010).

Appendix A. Supplementary data

Supplementary data to this article can be found online at https://doi.org/10.1016/j.ejmech.2021.113671.

References

[1] J.M. Llovet, R.K. Kelley, A. Villanueva, A.G. Singal, E. Pikarsky, S. Roayaie, R. Lencioni, K. Koike, J. Zucman-Rossi, R.S. Finn, Hepatocellular carcinoma, Nat. Rev. Dis. Primers. 7 (2021) 6.

[2] J.M. Llovet, S. Ricci, V. Mazzaferro, P. Hilgard, E. Gane, J.F. Blanc, A.C.d. Oliveira, A. Santoro, J.L. Raou, A. Forner, M. Schwartz, C. Porta, S. Zeuzem, L. Bolondi, T.F. Greten, P.R. Galle, J.F. Seitz, I. Borbath, D. Häussinger, T. Giannaris, M. Shan, M. Moscovici, D. Voliotis, J. Bruix, Sorafenib in advanced hepatocellular carcinoma, N. Engl. J. Med. 359 (2008) 378–390.

[3] W.Y. Lu, H.J. Li, Q.Y. Li, Y.C. Wu, Application of marine natural products in drug research, Bioorg. Med. Chem. 35 (2021) 116058.

[4] K. Zhang, F. Lai, S. Lin, M. Ji, J. Zhang, Y. Zhang, J. Jin, R. Fu, D. Wu, H. Tian, N. Xue, L. Sheng, X. Zou, Y. Li, X. Chen, H. Xu, Design, synthesis, and biological evaluation of 4-methyl quinazoline derivatives as anticancer agents simultaneously targeting phosphoinositide 3-kinases and histone deacetylases, J. Med. Chem. 61 (2019) 6992–7014.

[5] P.A. Haile, L.N. Casillas, B.J. Votta, G.Z. Wang, A.K. Charnley, X. Dong, M.J. Bury, J.J. Romano, J.F. Mehlmann, B.W. King, K.F. Erhard, C.R. Hanning, D.B. Lipshutz, B.M. Desai, C.A. Capriotti, M.C. Schaeffer, S.B. Berger, M.K. Mahajan, M.A. Reilly, R. Nagilla, E.J. Rivera, H.H. Sun, J.K. Kenna, A.M. Beal, M.T. Ouellette, M. Kelly, G. Stemp, M.A. Convery, A. Vossenkamper, T.T. MacDonald, P.J. Gough, J. Bertin, R.W. Marquis, Discovery of a first-in-class receptor interacting protein 2 (RIP2) kinase specific clinical candidate, 2((4-(Benzo[*d*]thiazol-5-ylamino)-6- (*tert*-butylsulfonyl)quinazolin-7-yl)oxy)ethyl dihydrogen phosphate, for the treatment of inflammatory diseases, J. Med. Chem. 62 (2019) 6482–6494.

[6] A. Lupien, C.S. Foo, S. Savina, A. Vocat, J. Piton, N. Monakhova, A. Benjak, D.A. Lamprecht, A.J.C. Steyn, K. Pethe, V.A. Makarov, S.T. Cole, New 2-Ethylthio-4-methylaminoquinazoline derivatives inhibiting two subunits of cytochrome *bc1* in *Mycobacterium tuberculosis*, PLoS Pathog. 16 (2020) 1008270–1008288.

[7] S. Lin, J. Jin, Y. Liu, H. Tian, Y. Zhang, R. Fu, J. Zhang, M. Wang, T. Du, M. Ji, D. Wu, K. Zhang, L. Sheng, Y. Li, X. Chen, H. Xu, Discovery of 4-methylquinazoline based PI3K inhibitors for the potential treatment of idiopathic pulmonary fibrosis, J. Med. Chem. 62 (2019) 8873–8879.

[8] T. Froehlich, C. Reiter, M.M. Ibrahim, J. Beutel, C. Hutterer, I. Zeittraeger, H. Bahsi, M. Leidenberger, O. Friedrich, B. Kappes, T. Efferth, M. Marschall, S.B. Tsogoeva, Synthesis of novel hybrids of quinazoline and artemisinin with high activities against plasmodium falciparum, human cytomegalovirus, and leukemia cells, ACS Omega 2 (2017) 2422–2431.

[9] X.Q. Zhang, X.F. Mou, N. Mao, J.J. Hao, M. Liu, J.Y. Zheng, C.Y. Wang, Y.C. Gu, C.L. Shao, Design, semisynthesis, α-glucosidase inhibitory, cytotoxic, and antibacterial activities of *p*-terphenyl derivatives, Eur. J. Med. Chem. 146 (2018) 232–244.

[10] X.M. Hou, T.M. Liang, Z.Y. Guo, C.Y. Wang, C.L. Shao, Discovery, absolute assignments, and total synthesis of asperversiamides A-C and their potent activity against *Mycobacterium marinum*, Chem. Commun. 55 (2019) 1104–1107.

[11] X.M. Hou, Y.Y. Li, Y.W. Shi, Y.W. Fang, R. Chao, Y.C. Gu, C.Y. Wang, C.L. Shao, Integrating molecular networking and ^{1}H NMR to target the isolation of chrysogeamides from a library of Marine-Derived Penicillium fungi, J. Org. Chem. 84 (2019) 1228–1237.

[12] R. Chao, X.M. Hou, W.F. Xu, Y. Hai, M.Y. Wei, C.Y. Wang, Y.C. Gu, C.L. Shao, Targeted isolation of asperheptatides from a Coral-Derived fungus using LC-MS/MS-Based molecular networking and antitubercular activities of modified cinnamate derivatives, J. Nat. Prod. 84 (2021) 11–19.

[13] C.S. Li, C.Y. An, X.M. Li, S.S. Gao, C.M. Cui, H.F. Sun, B.G. Wang, Triazole and dihydroimidazole alkaloids from the marine sediment-derived fungus *Penicillium paneum* SD-44, J. Nat. Prod. 74 (2011) 1331–1334.

[14] H.Y. Lee, J.Y. Chang, C.Y. Nien, C.C. Kuo, K.H. Shih, C.H. Wu, C.Y. Chang, W.Y. Lai, J.P. Liou, 5-Amino-2-aroylquinolines as highly potent tubulin polymerization inhibitors. Part 2. The impact of bridging groups at position C-2, J. Med. Chem. 54 (2011) 8517–8525.

[15] Y.S. Tung, M.S. Coumar, Y.S. Wu, H.Y. Shiao, J.Y. Chang, J.P. Liou, P. Shukla, C.W. Chang, C.Y. Chang, C.C. Kuo, T.K. Yeh, C.Y. Lin, J.S. Wu, S.Y. Wu, C.C. Liao, H.P. Hsieh, Scaffold-hopping strategy: synthesis and biological evaluation of 5,6-fused bicyclic heteroaromatics to identify orally bioavailable anticancer agents, J. Med. Chem. 54 (2011) 3076–3080.

[16] B.L. Flynn, G.S. Gill, D.W. Grobelny, J.H. Chaplin, D. Paul, A.F. Leske, T.C. Lavranos, D.K. Chalmers, S.A. Charman, E. Kostewicz, D.M. Shackleford, J. Morizzi, E. Hamel, M.K. Jung, G. Kremmidiotis, Discovery of 7-hydroxy-6-methoxy-2-methyl-3-(3,4,5-trimethoxybenzoyl)benzo[*b*]furan (BNC105), a tubulin polymerization inhibitor with potent antiproliferative and tumor vascular disrupting properties, J. Med. Chem. 54 (2011) 6014–6027.

[17] Y.P. Zhu, Z. Fei, M.C. Liu, F.C. Jia, A.X. Wu, Direct one-pot synthesis of luotonin F and analogues via rational logical design, org. Lett. 15, 2013, pp. 378–381.

[18] T.B. Nguyen, J.Y. Hou, P. Retailleau, Sulfur-promoted synthesis of 2-aroylquinazolin-4(3*H*)-ones by oxidative condensation of anthranilamide and acetophenones, Adv. Synth. Catal. 361 (2019) 3337–3341.

[19] A. Shergalis, D. Xue, F.Z. Gharbia, H. Driks, B. Shrestha, A. Tanweer, K. Cromer, M. Ljungman, N. Neamati, Characterization of aminobenzylphenols as protein disulfide isomerase inhibitors in glioblastoma cell lines, J. Med. Chem. 63 (2020) 10263–10286.

[20] H. Liu, Q. Fu, Y. Lu, W. Zhang, P. Yu, Z. Liu, X. Sun, Anti-tubulin agent vinorelbine inhibits metastasis of cancer cells by regulating epithelial-mesenchymal transition, Eur. J. Med. Chem. 200 (2020) 112332–112340.

[21] J. Yang, S. Hu, C. Wang, J. Song, C. Chen, Y. Fan, Y. Ben-David, W. Pan, Fangchinoline derivatives induce cell cycle arrest and apoptosis in human leukemia cell lines via suppression of the PI3K/AKT and MAPK signaling pathway, Eur. J. Med. Chem. 186 (2020) 111898–111908.

[22] Q.K. Shen, H. Deng, S.B. Wang, Y.S. Tian, Z.S. Quan, Synthesis, and evaluation of *in vitro* and *in vivo* anticancer activity of 14-substituted oridonin analogs: a novel and potent cell cycle arrest and apoptosis inducer through the p53-MDM2 pathway, Eur. J. Med. Chem. 173 (2019) 15–31.

[23] B. Li, Y. Li, C. Tomkiewicz-Raulet, P. Dao, D. Lietha, E. Yen-Pon, Z. Du, X. Coumoul, C. Garbay, M. Etheve-Quelquejeu, H. Chen, Design, synthesis, and biological evaluation of covalent inhibitors of focal adhesion kinase (FAK) against human malignant glioblastoma, J. Med. Chem. 63 (2020) 12707–12724.

[24] T.A. Elwaie, S.E. Abbas, E.I. Aly, R.F. George, H. Ali, N. Kraiouchkine, K.S. Abdelwahed, T.E. Fandy, K.A. El Sayed, Z.Y. Abd Elmageed, H.I. Ali, HER2 kinase-targeted breast cancer therapy: design, synthesis, and *in vitro* and *in vivo* evaluation of novel lapatinib congeners as selective and potent HER2 inhibitors with favorable metabolic stability, J. Med. Chem. 63 (2020) 15906–15945.

[25] P. Wang, Q. Gong, J. Hu, X. Li, X. Zhang, Reactive oxygen species (ROS)-Responsive prodrugs, probes, and theranostic prodrugs: applications in the ROS-related diseases, J. Med. Chem. 64 (2021) 298–325.

[26] J.P.C. Coverdale, H.E. Bridgewater, J.I. Song, N.A. Smith, N.P.E. Barry, I. Bagley, P.J. Sadler, I. Romero-Canelon, *In vivo* selectivity and localization of reactive oxygen species (ROS) induction by osmium anticancer complexes that circumvent platinum resistance, J. Med. Chem. 61 (2018) 9246–9255.